IUCr 2011. XAFS Tutorial for Crystallographers.
Madrid August 22
XAFS Theory: XANES and EXAFS Spectra.
Recent advances in synchrotron techniques, new opportunities in organometallic materials, complex phase systems and cluster studies.
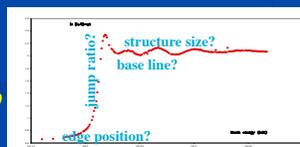
Chris. Chantler

Assoc. Prof. & Reader, FAIP
University of Melbourne
Victoria 3010, Australia
chantler@unimelb.edu.au
http://optics.ph.unimelb.edu.au/~chantler/home.html

XAFS Theory: XANES and EXAFS Spectra

1. Why XAFS?
2. What is XAFS?
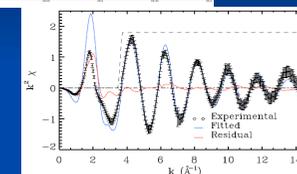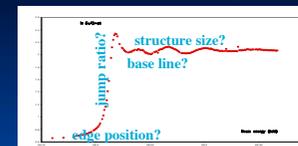3. How does XAFS work?
   Difficulties
   Links with Crystallography
   Realisation: A: Absorption
   Realisation: B: Fluorescence
4. Past, present and future...
Recent advances in synchrotron techniques, new opportunities in organometallic materials, complex phase systems and cluster studies.

XAFS Theory: XANES and EXAFS Spectra

1. Why XAFS?

- Crystallography - periodicity, symmetry and mean structure of perfect crystals [X-ray; Electron Diffraction; Neutron Diffraction]
- Nanocrystallites in advanced synchrotron beams; or [X-ray] Powder Diffraction
- TEM etc. of surfaces or slices [destructive].
- Great difficulties for disordered systems; solutions; dilute systems; local order; dynamic bond lengths; active centres.
- X-ray Absorption Fine Structure [XAFS] deals directly with these questions and more.
- Complementary for complex systems, organometallics, bioactive systems, ideal crystals or metals

---

XAFS Theory: XANES and EXAFS Spectra

1. Why XAFS?

- **Recent advances in synchrotron techniques,**
- **new opportunities in organometallic materials,**
- **dynamic bond investigation,**
- **thermal dependence of structure [especially disordered],**
- **complex phase systems**
- **cluster studies**
- **12000 papers in the last 5 years.**

XAFS Theory: XANES and EXAFS Spectra
2. What is XAFS?

X-ray Absorption Fine Structure [XAFS] is the sequence of sharp oscillations in the Absorption coefficient just above the absorption edge for a particular sub-shell [K, LI, LII, LIII, M...] of an element [Fe, Cu, Ni, C, Mo, Au, ...] in a material, corresponding to the creation of electron holes in the 1s, 2s, 2p1/2, 2p3/2 etc. atomic subshells.

The material may be an ideal crystal or metal, a nanocrystal or powder, or a non-ideal mixture or dilute solution.

For detailed background, see IUCr Commission on XAFS Definitions: http:// www.iucr.org/resources/commissions/xafs/xafs-related-definitions-for-the-iucr-dictionary

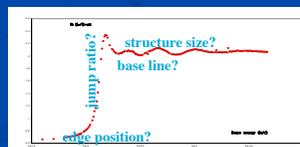*See also: http://www.iucr.org/ for feature*

THIS CONGRESS: MS16, MS33, MS42, MS56,

MS70, KN27, [Sunday]: MS77 [XAFS Developments]

Bourke [Sunday, MS76], MS91

Posters Thur/Fri: Rae [Abstract 582, MS56.P03]

Chantler [Abstracts 524, MS42.P02]

structure size?
base line?
edge position?

XAFS Theory: XANES and EXAFS Spectra
2. What is XAFS?

- X-ray Absorption Fine Structure (XAFS): modulation of the absorption coefficient at & above an Absorption Edge of an element due to chemical state & structure of immediate surroundings. Commonly divided into 'near edge' region (XANES or NEXAFS) to ~50 eV above the absorption edge & 'extended' region (EXAFS) giving oscillations in the absorption coefficient from ~50 eV.
- XANES (X-ray Absorption Near Edge Spectroscopy) for X-ray edges (~1 keV and above); NEXAFS (Near-edge X-ray Absorption Fine Structure) for soft X-ray edges.
- Spectral features before the main absorption edge - 'pre-edge' features - are associated with transitions to bound states.

XAFS Theory: XANES and EXAFS Spectra
2. What is XAFS?

X-ray Absorption Spectroscopy (XAS) is a technique for measuring the linear absorption coefficient $\mu(E)$ of a substance as a function of the incident photon energy E in the X-ray regime. This technique is element & orbital-specific & determines the local atomic & electronic structure of matter. XAS conventionally includes techniques of XAFS, which in turn includes both XANES & EXAFS. An XAS spectrum may also be obtained using fluorescence, electron yield & scattering processes indirectly (i.e. without directly measuring the absorption of X-rays).

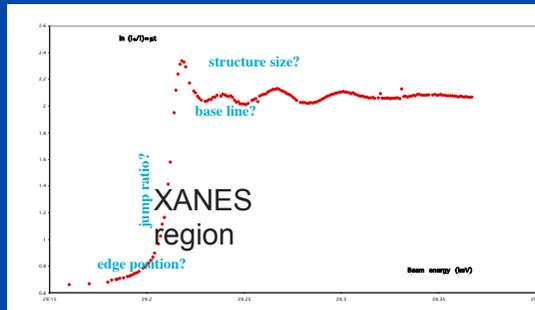## XAFS Theory: XANES and EXAFS Spectra
2. What is XAFS?

XANES (X-ray Absorption Near-Edge Structure) is represented by pre-edge features from bound-bound transitions in the molecular structure around the target element, which is a reflection of the Fermi level & Fermi surface. If the region of the target atom is depleted of electrons, representing ionic bonding & positive cations, then additional pre-edge spectral lines are likely to ensue. Conversely, if the target atom is negatively charged, the Fermi level will rise and pre-edge features may disappear. Discrete transitions often have a particular symmetry & polarity, so that pre-edge features may appear or disappear in particular polarisations of the incident X-ray field; or for particular coordination of the nearest neighbours of the target atom (two-fold, linear or bent; square planar or tetrahedral; etc.)

XAFS Theory: XANES and EXAFS Spectra
2. What is XAFS?

XANES is often used qualitatively to evaluate charge state, bonding symmetry & coordination of a central atom; or by comparison to a series of empirical standards to evaluate the likely molecular species & surroundings of a target ion.

XAFS Theory: XANES and EXAFS Spectra
2. What is XAFS?

XANES: Ideal examples and archetypes:
charge state, bonding symmetry and coordination of a central atom; or by comparison to a series of empirical standards to evaluate the likely molecular species and surrounding of a target atom or ion.

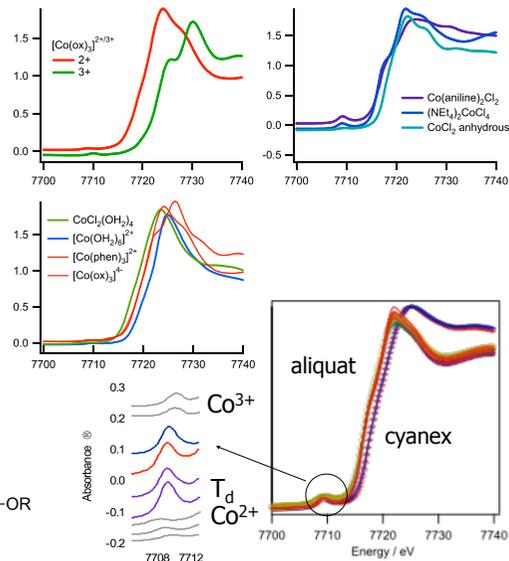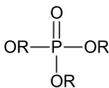## Metal Transport

Best. Cheah

Feed stream Impure Co^{2+}

Extract stream Pure Co^{2+}

Polymer: CTA
Extractant: cyanex

XAFS Theory: XANES and EXAFS Spectra
2. What is XAFS?

The Extended X-ray Absorption Fine Structure (EXAFS) (q.v.) region contains modulation of the absorption coefficient that can be interpreted in terms of photo-electron scattering.

In relation to the (linear) absorption coefficient, the XAFS is defined as

$$\chi = \frac{\mu(E) - \mu_{free}(E)}{\mu_{free}(E)}$$

where μ_{free} is the (linear) absorption coefficient of the free atom, that is in the absence of any immediate surroundings and chemical modifications. The XAFS is often practically defined as
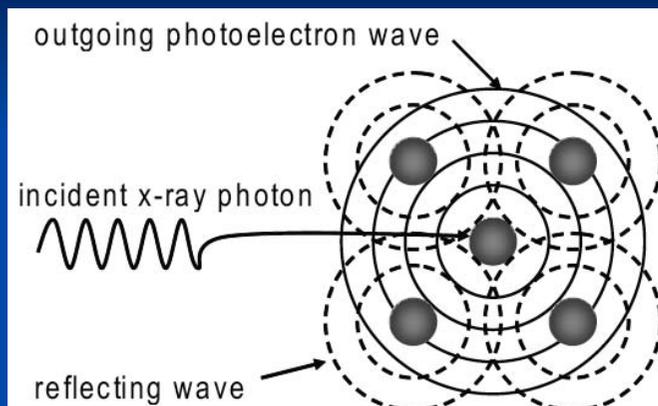
$$\chi = \frac{\mu_{measured}(E) - \mu_{ref}(E)}{\mu_{ref}(E)} \quad \text{or} \quad \chi = \frac{\mu_{measured}(E) - \mu_0(E)}{\Delta\mu} \quad \text{instead.}$$

where $\mu_{measured}$ is the measured linear absorption (typically from the ratio of ion chamber intensities, possibly normalised for some experimental errors), and μ_{ref} is a reference background spectrum simulating aspects of both the edge and a pseudo-atomic state. In the third approach, μ_0 is a smooth mathematical background function through $\mu_{measured}$ (e.g. a spline fit) and the XAFS is normalized by $\Delta\mu$ the 'edge jump' at the Absorption edge in $\mu_{measured}$. Naturally, these different definitions can give variations in μ where the normalisations might differ significantly, especially if their differences vary with energy.

Slide 1 (top-left)

outgoing photoelectron wave

incident x-ray photon

reflecting wave

Slide 2 (top-right)

O, H, H

structure size?
base line?
jump ratio?
edge position?

Au L$_I$-edge
ANBF 20B 2000

Sn K-edge
BESSRC 12BM 2001

Ag K-edge
SRI-CAT 1BM 1999

Slide 3 (bottom-left)

$$\chi(k) = \frac{[\mu/\rho](E) - [\mu_0/\rho](E)}{[\mu_0/\rho](E)}$$

$$k = \frac{2\pi}{h}\sqrt{2m_e(E - E_0)}$$

E_0 = 20,008 eV
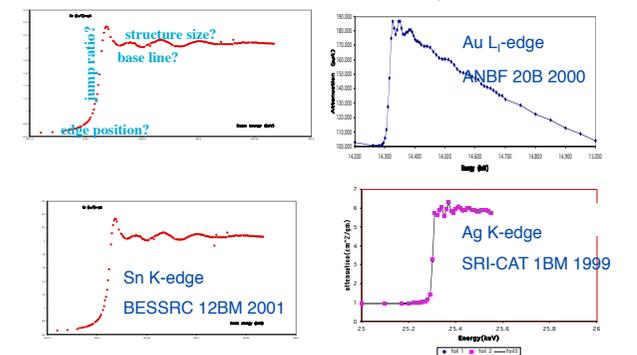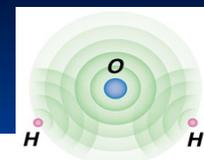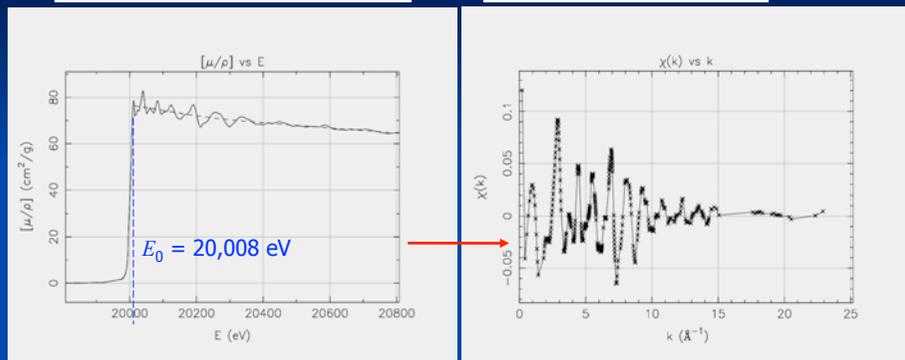
Mass Attenuation Coefficients (solid)
Background Atom-Like Mass
Attenuation (dashed)
M. D. de Jonge, C. Q. Tran, C. T. Chantler, Z. Barnea, B. B. Dhal, D. J. Cookson, W.-K. Lee, A. Mashayekhi, Phys. Rev. A 71, 032702 (2005) 032702-1-16

Isolated XAFS Spectrum
(Error bars smaller than width of line)
L. F. Smale, C. T. Chantler, M. D. de Jonge, Z. Barnea, C.Q. Tran, Radiation Physics & Chemistry 75 (2006) 1559-1563

Slide 4 (bottom-right)

- Fine Structure observed 1920s. LRO/SRO theory Kronig (1931/1932)
- Imaginary component & function needed for dynamical diffraction theory (Zachariasen 1945)
- Bijvoet ratios, absolute configurations & phasing (1949)
- Fourier Transform approach to EXAFS (Sayers 1971)
- Spherical wavelets Rehr (2000) Muffin-tin
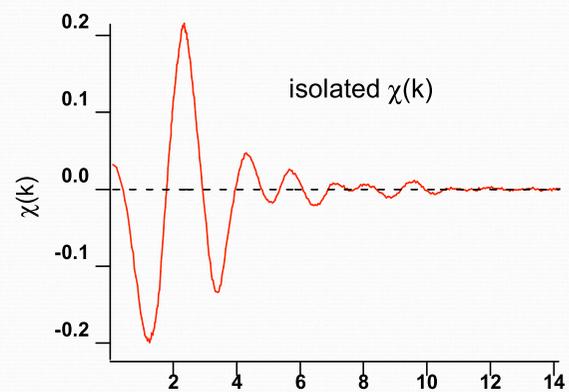- Recent techniques e.g. Joly, Benfatto, Soldatov, Chantler

Data reduction
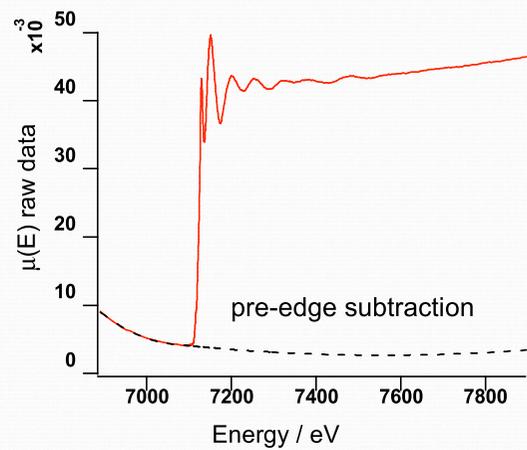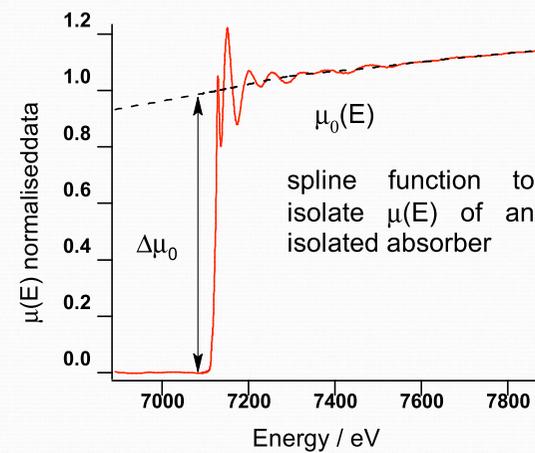
FT intensity vs R / Å
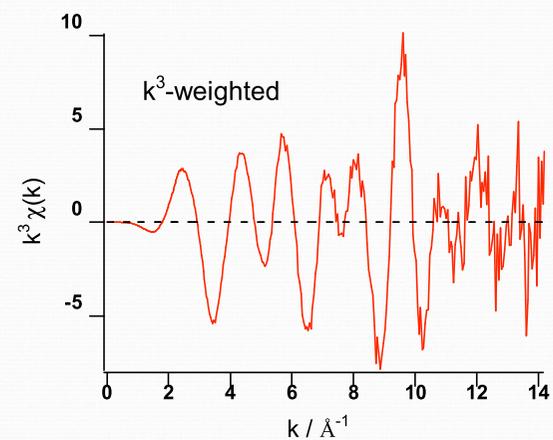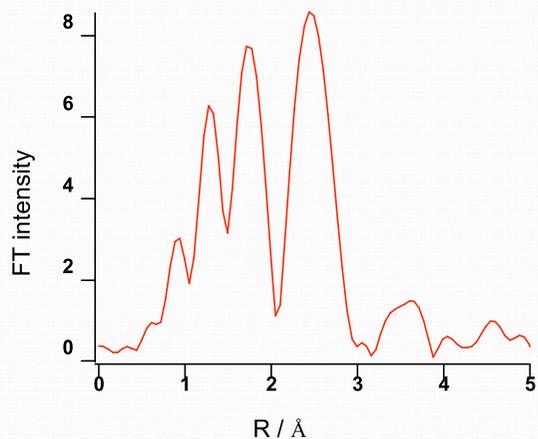
XAFS Theory: XANES and EXAFS Spectra

3. How does XAFS work?
Lots of structure (even at room temperature)
Lots of spectral features
If a theory can predict these, it can fit for unknown coordination, bond lengths, etc...

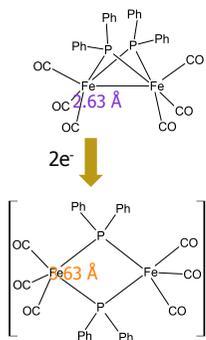
Fe$_2$(μ-PPh$_2$)$_2$(CO)$_6$
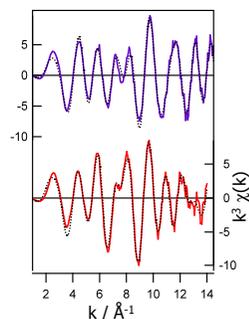
Stephen P Best, Michael Cheah

Phosphido-Bridged Diiron Compounds

❑ Reduction product highly air sensitive although structure known

SP Best et al., Inorg. Chem., **2004**, 43, 5635.

Ph Ph
Ph—P   P   CO
OC—Fe—Fe—CO
OC 2.63 Å CO
OC CO

2e⁻

[structure]²⁻

Fe-Fe / Å	Fe-P / Å	R(%) {χ²}
2.61	**2.21**	11.35
[2.63]	[2.21]	{2.80}
(0.0007)	(0.0009)	
3.58	**2.26**	9.22
[3.63]	[2.29]	{1.48}
(0.0060)	(0.0034)	

BL 20 B, Photon Factory
Data analysis: XFit
N$_{refined}$ = 16, N$_{idp}$ = 26

Ginsburg *et. al. JACS,* **1979,** 101, 6550.

XAFS of **H$_2$DP**

SPB/MC- 4

observed
calculated No Fe-H
calculated refined Fe-H
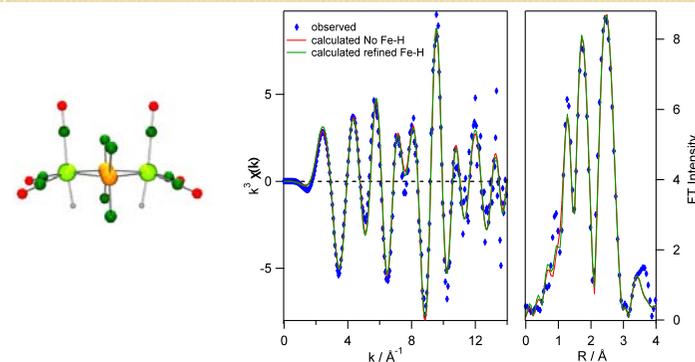
Data	H$_2$:DP		
	No Fe-H	Fixed Fe-H	Refined Fe-H
χ² (R$_{EXAFS}$/%)	2.11 (13.22)	1.68 (11.80)	1.62 (11.58)
Fe-Fe/Å	3.62	3.62	3.62
Fe-μ-P/Å	2.26	2.26	2.26

More significantly: Changes in heavy atom distances from EXAFS match calculations

Slide 1 (top-left)

Influence of Protonation on Fe-Fe

Simone Löscher,[†] Lennart Schwartz,[‡] Matthias Stein,[§] Sascha Ott,[*,‡] and Michael Haumann[*]

Cheah, M. H., Borg, S. J., and Best, S. P., *Inorg. Chem.* **2007**, *46*, 1741-50

$$1' \xrightarrow[\text{(1 eq)}]{\text{HOTf}} [1H]^+ \xrightarrow[\text{(excess)}]{\text{HOTf}} [1HHy]^{2+} \xrightarrow[\text{(excess)}]{\text{TEOA}} [1Hy]^+$$
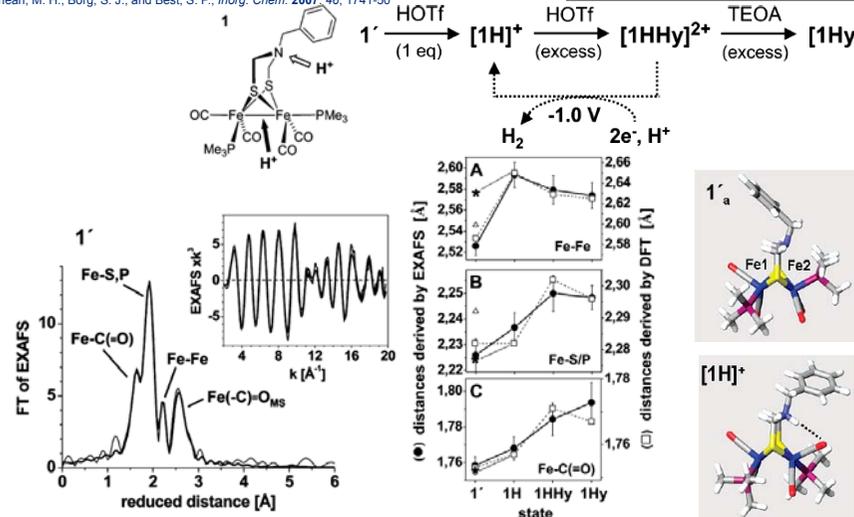
Borg, S. J., Bondin, M. I., Best, S. P., Razavet, M., Liu, X., Pickett, C. J., *Biochem. Soc. Trans.* **2005**, *33*, 3-6

Borg, S. J., Tye, J. W., Hall, M. B., Best, S. P., *Inorg. Chem.* **2007**. *46*, 384-394

Slide 2 (top-right)

XAFS of the Cr(VI)-Glutathione Complex
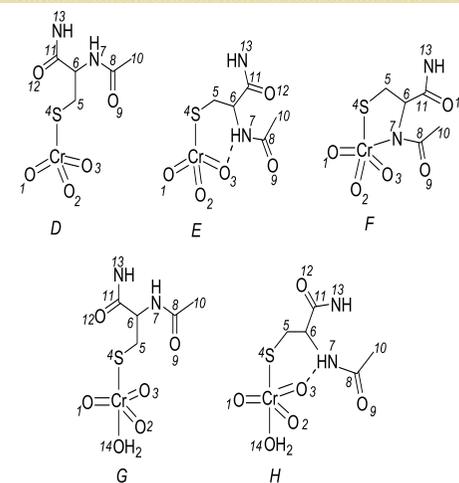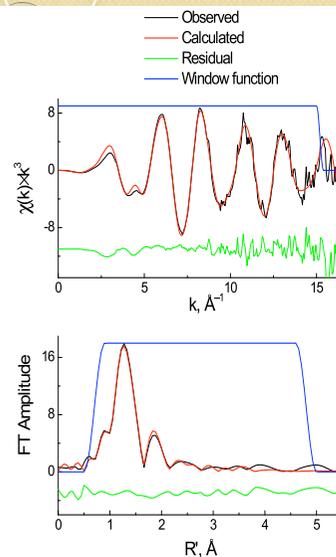
Levina, A.; Lay, P. A. *Inorg. Chem.* 2004, *43*, 324-335.

Slide 3 (bottom-left)

XAFS of a Cr(V) Glutathione Complex
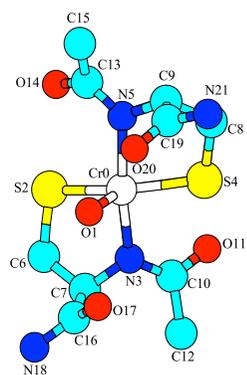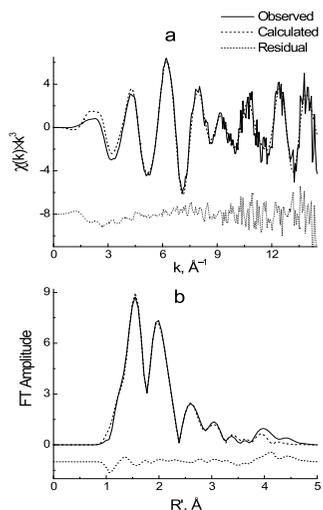
Levina, A.; Zhang, L.; Lay, P. A. *Inorg. Chem.* 2003, *42*, 767-784.

Slide 4 (bottom-right)

Eu[III] speciation in hydrothermal chloride solutions

Weihua Liu, Stacey Borg… CSIRO Exploration & Mining, Australia
Barbara Etschmann, Joël Brugger… U Adelaide & South Australian Museum
Michael Cheah… ANBF, Photon Factory, KEK, Japan

- Structures of main Eu chloride (aq) species ?
- Thermodynamic properties?
- Require collection of X-ray absorption spectra from Eu(III) in chloride solutions between 25-150 °C.

Eu speciation
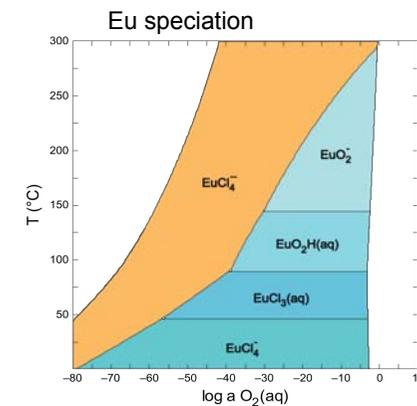
XAFS Analysis

Sample	No. of ligands	bond distance (Å)	σ^2
Solution A: 0.07 m EuCl$_3$ in water at 25°C	O: 9 (fixed)	2.41±0.02	0.006
Solution B: 0.07 m EuCl$_3$ in 15 m LiCl at 150°C	O: 6 (fixed) Cl: 3 (fixed)	2.38±0.05 2.68±0.04	0.008 0.01

[FeFe]-Hydrogenase

'H-cluster'

$\{2Fe\}_{H-ox}$

$\{2Fe\}_{H-red}$

H-ox

H-red

$\nu(CN)$

$\nu(CO)_{term}$

$\nu(CO)_{bridge}$

C≡N

Peters *et al. Science* **1998**.
Fontecilla-Camps *et al. Structure,* **1999**.

De Lacey *et al., JACS,* **2000**.
Albracht *et al., Eur. J. Biochem.,* **1996** & **1998**.

EXAFS models: Fe$_2$S$_2$(CO)$_6$
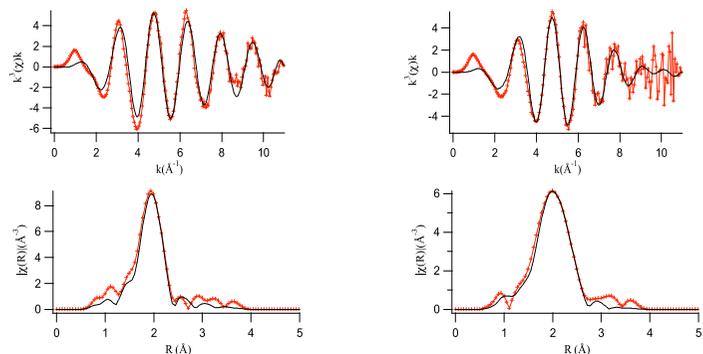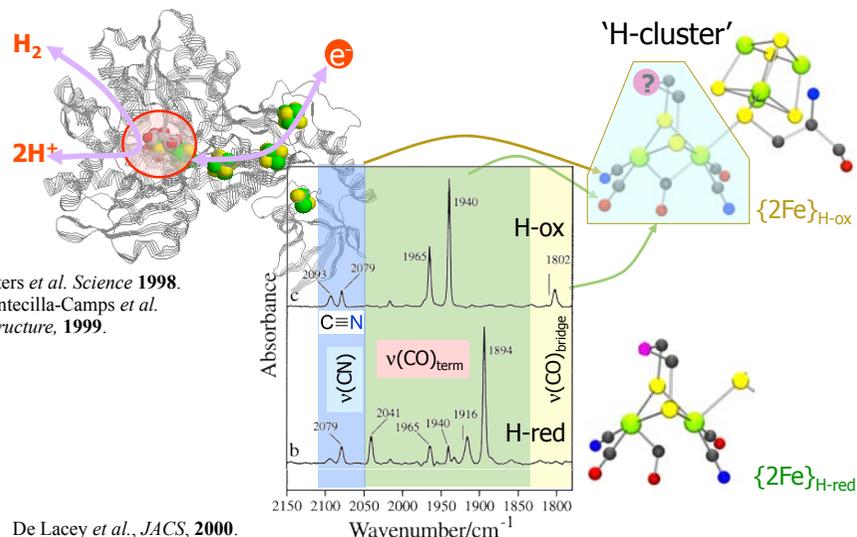
Cheah, M. H., Tard, C., Borg, S. J., Liu, X., Ibrahim, S. K., Pickett, C. J. and Best, SP, J. Amer. Chem. Soc., **2007**, 129, 11085-11092.

Borg, SJ, Behrsing, T, Best, SP, Razavet, M, Liu, XM, Pickett, CJ, *J. Amer. Chem. Soc.* 126 (2004) 16988-16999

Fe-Fe / Å	Fe-S / Å	Fe-C / Å	Fe--O / Å
2.49 [2.51]	2.24 [2.25]	1.80 [1.80]	2.95 [2.94]

$C_{2v}F$
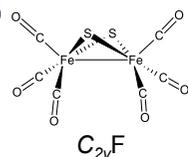
$N_{idp}/N_{p(model)}$ = 1.3
R = 11.25 %
χ^2 = 2.82

$C_{2v}P$
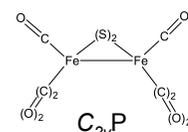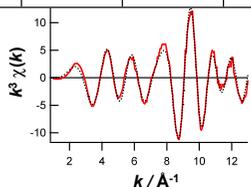
$N_{idp}/N_{p(model)}$ = 1.5
R = 12.37 %
χ^2 = 3.41

$C_{2v}P_s$
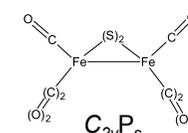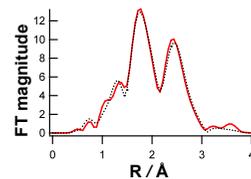
$N_{idp}/N_{p(model)}$ = 2.3
R = 9.93 %
χ^2 = 2.20

$C_{2v}Z$
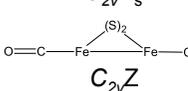
$N_{idp}/N_{p(model)}$ = 2.7
R = 13.24 %
χ^2 = 3.93

Structure of "3B" – Type Product

3S

"3B"

Stacey Borg + Mark Bondin

Aust J Chem **2006**, *59*, 263.

	3S	"B"
Fe-S	2.241	2.253 Å
Fe-C	1.786	1.772 Å
Fe-Fe	**2.485**	**2.527 Å**

⇒ Retention of Fe-Fe bond ?
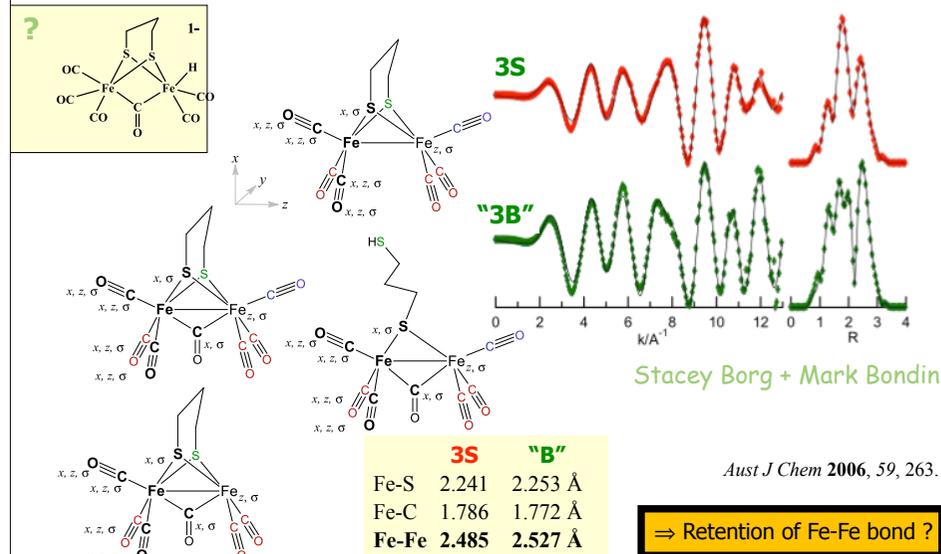
3. How does XAFS work?

Local Structure Guess
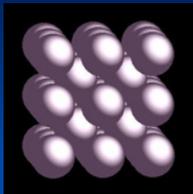
Metallic Molybdenum:
BCC Crystal

Model of XAFS Spectrum (XAFS Equation)

Program?

$$\chi_{th}(k) = \sum_j N_j S_0^2 F_j(k) \frac{\sin(2kr_j + \phi_j(k))}{kr_j^2} e^{-2\sigma_j^2 k^2} e^{-2r_j/\lambda_j(k)}$$

$$r_j = (1+\alpha)r_{0,j}$$

Expansion Coefficient

Backscattering Amplitude and Phase

Many Body Reduction Factor

Mean Free Path

Debye-Waller Factor

Distance To Coordination Shell Based On Input

Coordination Numbers

k 'photoelectron momentum index' cf physical momentum.
$\chi(k)$ is dimensionless: F in units of 1/k (i.e. length)
Other definitions for F being dimensionless (as a form factor or scattering amplitude)
have (kR)^2 in the denominator to maintain consistency of units.

XAFS Theory: XANES and EXAFS Spectra
3. How does XAFS work?

$$\chi_{th}(k) = \sum_j N_j S_0^2 F_j(k) \frac{\sin(2kr_j + \phi_j(k))}{kr_j^2} e^{-2\sigma_j^2 k^2} e^{-2r_j/\lambda_j(k)}$$

$$r_j = (1+\alpha)r_{0,j}$$

Sum over *shells* of a particular atom type *j* & distances from the origin of the initial photoelectron.

N_j : coordination number, r_j : interatomic distance, σ^2_j : mean-square disorder in distance for j^{th} shell.

F_j : photoelectron (back-)scattering amplitude, $\Phi_j(k)$: (back-)scattering phase for the jth atomic shell.

S_0^2: amplitude reduction factor (relaxation of the absorbing atom due to the presence of the empty core level and Multi-Electron Excitations).

$\lambda_j(k)$: photoelectron inelastic mean free path - strong dependence upon *k*, range 1 - 100 Å over XAFS

IUCr 2011. XAFS Tutorial. C.T. Chantler

XAFS Theory: XANES and EXAFS Spectra
3. How does XAFS work?

$$\chi_{th}(k) = \sum_j N_j S_0^2 F_j(k) \frac{\sin(2kr_j + \phi_j(k))}{kr_j^2} e^{-2\sigma_j^2 k^2} e^{-2r_j/\lambda_j(k)}$$

$$r_j = (1+\alpha)r_{0,j}$$

Crude approximation of $\Phi_j(k) \approx -2\, a_0 k$ (a_0 : Bohr radius) works for many systems: peaks for a particular shell in Fourier transform of $\chi(k)$ shifted ~ 0.5 Å below actual interatomic distance.
$F_j(k)$ & $\Phi_j(k)$ depend upon *Z* of scattering atom, with non-linear dependence on *k*.
exp(-2k$^2\sigma_j^2$) : EXAFS isotropic or effective Debye-Waller Factor, including thermal vibration & static disorder. Sum over shells and σ_j^2 in the standard EXAFS equation can be generalized to an integral over the partial pair distribution function *g(R)* in which one atom is always the absorbing atom.

IUCr 2011. XAFS Tutorial. C.T. Chantler

XAFS Theory: XANES and EXAFS Spectra
3. How does XAFS work?

$$\chi_{th}(k) = \sum_j N_j S_0^2 F_j(k) \frac{\sin(2kr_j + \phi_j(k))}{kr_j^2} e^{-2\sigma_j^2 k^2} e^{-2r_j/\lambda_j(k)}$$

$$r_j = (1+\alpha)r_{0,j}$$

Sum can be generalized to be over photo-electron *scattering paths* instead of *shells of atoms*. This allows inclusion of multiple scattering paths for the photo-electron, giving important contributions. The interpretation of the EXAFS Equation is then slightly modified:
r_j is then half the path length; $F_j(k)$ and $\Phi_j(k)$ become (multiple) scattering amplitudes and phase-shifts for the entire path.
The EXAFS Equation allows the numerical determination of the local structural parameters N_j, r_j, σ_j^2 knowing the scattering amplitude $F_j(k)$ and $\Phi_j(k)$ for a small number (typically 1 to 10) of shells or paths. Theory normally breaks down at low *k* (the XANES region) as the *1/k* term increases, $\lambda_j(k)$ increases, the disorder terms do not strongly dampen the EXAFS, and the EXAFS picture of single particle scattering is no longer a good approximation.

IUCr 2011. XAFS Tutorial. C.T. Chantler

3. How does XAFS work?

$$\chi_{th}(k) = \sum_j N_j S_0^2 F_j(k) \frac{\sin(2kr_j + \phi_j(k))}{kr_j^2} e^{-2\sigma_j^2 k^2} e^{-2r_j/\lambda_j(k)}$$

$$r_j = (1+\alpha)r_{0,j}$$

- Lytle, F. W., 1999, J. Synchrotron Radiat. 6, 123
- Stumm von Bordwehr, R., 1989, Ann. Phys. (Paris) 14, 377.
- EXAFS Scattering Theory: Sayers, Stern, Lytle, Phys. Rev. Lett. 27 (1971) 1204
- Rehr, Albers, Rev. Mod. Phys. 72 (2000) 621-654
- Newville, M. (2004). *Fundamentals of XAFS. CARS, University of Chicago, Chicago IL*, pp. 23–24
- Bunker, G. (2010). In *Introduction to XAFS: A practical guide to X-ray Absorption Fine Structure Spectroscopy*, pp. 92–95. CUP
- Chantler et al., J Synch. Rad. submitted

---

3. How does XAFS work?
Difficulties

$$\chi_{th}(k) = \sum_j N_j S_0^2 F_j(k) \frac{\sin(2kr_j + \phi_j(k))}{kr_j^2} e^{-2\sigma_j^2 k^2} e^{-2r_j/\lambda_j(k)}$$

$$r_j = (1+\alpha)r_{0,j}$$

Fermi level / Fermi Energy.
1) the energy of 50% probability of occupation, lying between the highest occupied level and the lowest unoccupied level, often defined as their average. If the energy level spectrum is a continuum (or almost a continuum) the three levels coincide. In a many-body approach, the Fermi level is the energy necessary for adding or subtracting a particle from the system. In XAS the Fermi level is below or at the first allowed transition.
2) In XAS, the **Fermi energy** dictates possible pre-edge features and explains the possibility or impossibility of open scattering channels adding to near-edge structure. When theoretical formalisms compute the Fermi energy, crucial for the XANES region, the quantum mechanical convergence is essential, whether atomic, cluster, or periodic boundary conditions are used. The lack of convergence for theoretical formalisms can at this time lead to systematic errors in the determination of the Fermi energy and corresponding pre-edge structure of order 1- 10 eV in the X-ray regime and should be considered carefully as this affects the interpretation of XAFS and XANES.

$$k = \frac{2\pi}{h}\sqrt{2m_e(E-E_0)}$$

$$\chi_{th}(k) = \sum_j N_j S_0^2 F_j(k) \frac{\sin(2kr_j + \phi_j(k))}{kr_j^2} e^{-2\sigma_j^2 k^2} e^{-2r_j/\lambda_j(k)}$$

$$r_j = (1+\alpha)r_{0,j}$$

Absorption threshold Definitions In the literature there is much confusion, even in modern papers, concerning the definition of the absorption threshold. The absorption threshold should indicate the first allowed transition in an absorption spectrum. Many definitions are used in common parlance. They yield very different values in analysis.
1. The energy at which the open continuum channel for photo-electric absorption becomes available, producing a continuum photo-electron. This has an exact value from theory, subject to convergence issues.
2. An (higher) energy at which a secondary (two-step) photo-ionization channel becomes energetically possible; more challenging to compute theoretically, and less easily separable in XAS;
3. Experimentally, the **absorption threshold** is sometimes defined as the inflection point in the first derivative of the experimental edge spectrum (the point of maximum slope on the rising edge for a particular sub-shell); this is a convenient marker but – a. it is source, beam-line, and band-width dependent; b. it is affected by pre-edge structure and the **Fermi level** due to contributions from bound-bound channels ; c. the experimental edge may contain two or more inflection points, and d. the determination depends upon instrumental resolution.
4. Experimentally, the **absorption threshold** is sometimes defined as the point exactly 50% of the jump ratio from the background absorption (from other shells, including scattering) to the peak absorption coefficient of the XAS spectrum, defined either by the clear maximum or by the smooth line representing the background to be subtracted in the determination of χ (k); this is problematic measure, since it depends upon beam-line dependent effects (3 above), and a wide variety of different predictions of the 'true background level' μ_0 above the edge.
5. Computationally, an **absorption threshold** is defined for XAFS fitting as E_0 which is either an arbitrary fitting coefficient or the starting point of the *k* transform, which in turn generates the Fourier transform for the XAFS structure χ(k); as the latter, it should be defined as per 1 above; as the former, this will often yield a function of *r* and errors in E_0 of order 10 eV or more which can result in bond length errors of order 0.02 Å or more. Computationally and experimentally, the energy axis is often not defined, so inconsistencies between these definitions are relatively common.

$$k = \frac{2\pi}{h}\sqrt{2m_e(E-E_0)}$$

$$\chi_{th}(k) = \sum_j N_j S_0^2 F_j(k) \frac{\sin(2kr_j + \phi_j(k))}{kr_j^2} e^{-2\sigma_j^2 k^2} e^{-2r_j/\lambda_j(k)}$$

$$r_j = (1+\alpha)r_{0,j}$$

Most theoretical approaches have great difficulty in experimental modelling at low k, which is one of the key reasons for standard analysis [fitting] to use both a window function (i.e. to fit over a restricted *k*-range) and a k^2 or k^3 weighting (to emphasise higher-*k* oscillations). Also, experimental uncertainties are not propagated.

Panel 1 (top left)
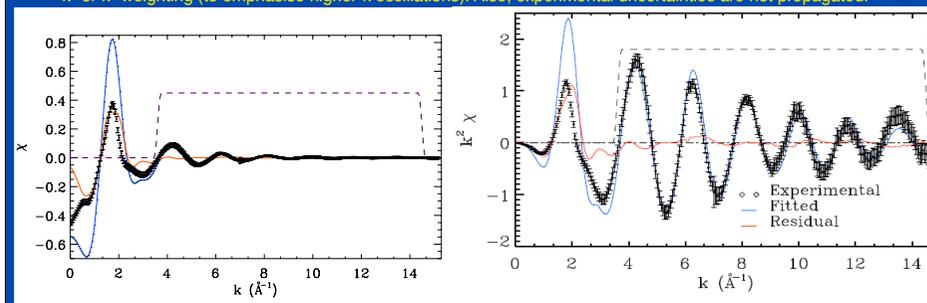
XAFS Theory: XANES and EXAFS Spectra
XAFS, XANES, XERT

- Quantitative X-ray Absorption in non-crystalline systems
- XANES: Oxidation state. Pre-edge bound features. Valence interactions. Chemical shifts.
- XAFS: Nearest-neighbour radius. Coordination number. Element (ionization state) of nearest neighbour. Phase offsets and amplitudes. *Active Centres. Reactive Intermediates*. Bonding, correlated motion.
- Scattering. Radiation safety, Medical imaging.
- Fundamental parameters: Atomic & condensed matter theory & quantum chemistry. Complex form factor.
- Applications: Chemistry, Biology, Biomedicine, Earth Sciences, Spectroscopy, Mineralogy, Engineering, Physics *[Lay, Best, Brugger, Bradley, Creagh, Rubio, Ascone, Feiters, Joly...]*

Panel 2 (top right)

Links: X-ray Absorption Fine Structure and Crystallography *(X-RAY) ATOMIC FORM FACTOR:* Resonant scattering amplitude of X-rays by charge (electron) density

$$\mathrm{Re}(f) = f_0 + f' + f_{NT}, f' = f_1 + f_{rel} - Z$$

$$f_0(q,Z) = 4\pi \int_0^\infty \frac{\rho(r)\sin(qr)r^2 dr}{qr}$$

$$f'(E,Z) = f'(\infty) - \frac{2}{\pi} P \int_0^\infty \frac{\varepsilon' f''(\varepsilon')}{E^2 - (\varepsilon')^2} d\varepsilon'$$

$$\mathrm{Im}(f) = f''(E) = f_2(E) = \frac{E\mu_{PE}(E)}{2hcr_e}$$

'normal' coherent scattering factor

'anomalous' scattering factor

Utility: X-ray Diffraction experiments, Crystallography…

$$F(hkl) = \sum_j f_j e^{-M_j} e^{2\pi i(hx_j + ky_j + lz_j)}, (TDS = 0)$$

Electronic wavefunction distribution, bonding…

$$\Delta\rho(x,y,z) = \frac{1}{V}\sum_h \sum_k \sum_l \Delta F(hkl) e^{-2\pi i(hx+ky+lz)}$$

VUV research, multilayer modelling, critical angle spectroscopy…

$$n_r = n + ik = \sqrt{\varepsilon} = 1 - \delta - i\beta = 1 - \frac{r_0}{2\pi}\lambda^2 \sum_j n_j f_j \quad n_j \text{ atom number density; } r_0 \text{ classical electron radius}$$

Transmission, attenuation experiments…

$$\mu_{PE}(E) = f_2(E)2hcr_0 / E$$

Electron form factor (Mott-Bethe)…

$$f^B(q,Z) = \frac{me^2}{2\pi\hbar^2\varepsilon_0}\left\{\frac{Z - f(q,Z)}{q^2}\right\}$$

Panel 3 (bottom left)

Links: X-ray Absorption Fine Structure and Crystallography *ATTENUATION & THE (X-RAY) ATOMIC FORM FACTOR:* One Example of useage: FFAST:

$$\mu_{PE}(E) = f_2(E)2hcr_0 / E$$

$$[\mu_{PE}/\rho](E) = \sigma_{PE}/(uA)$$

$$\mathrm{Im}(f) = f''(E) = f_2(E) = \frac{E\mu_{PE}(E)}{2hcr_e}$$

$$\mathrm{Re}(f) = f_0 + f' + f_{NT}, f' = f_1 + f_{rel} - Z$$

$$f_0(q,Z) = 4\pi \int_0^\infty \frac{\rho(r)\sin(qr)r^2 dr}{qr}$$

http://physics.nist.gov/PhysRefData/FFast/Text/cover.html

Chantler, CT, Olsen, K, et al. (2005) X-Ray Form Factor, Attenuation & Scattering Tables (v2.1) [Online]; Chantler, CT, JPhysChemRefData 29(4), 597-1048 (2000); Chantler, CT, JPhysChemRefData 24, 71-643 (1995).

(NIST X-Ray Form Factor, Attenuation, and Scattering Database screenshot reproduced at right)

Panel 4 (bottom right)

XAFS Theory: XANES and EXAFS Spectra
3. How XAFS works - Realisation
A: Absorption

Absorption is conventionally given by the Beer-Lambert equation:

$$I = I_0 \exp\{-[\mu/\varrho][\varrho t]\}$$

I_0 is the incident X-ray beam intensity, I is the transmitted intensity, $[\mu/\varrho]$ is the X-ray mass absorption coefficient of the material for the energy of the X-ray beam, and t is the thickness of the foil. The beauty of this is that the negative values of the natural logarithms of the measured ratios of I/I_0,

$$-\ln\{I/I_0\} = [\mu/\rho][\rho t] = \mu t$$

plotted against t (or $[\varrho t]$), fall on a straight line with slope μ (linear absorption coefficient) (or $[\mu/\varrho]$). Hence the mass absorption coefficient, the photoelectric coefficients, the scattering components and the form factors of the material can be directly evaluated from the logarithm of the normalised ratio. This then gives the input spectrum for the extraction of the XAFS, XANES or EXAFS signal.

This requires careful correction for **detector efficiencies and air path** (Tran, C. Q., Chantler, C. T. & Barnea, Z. (2003). *Phys. Rev. Letts.* **90**, 257401–1–4), **scattering** (Tran, C. Q., Chantler, C. T., Barnea, Z. & de Jonge, M. D. (2004). *Rev.* Sci. Instrum. 75, 2943–2949), **harmonics** (Tran, C. Q., Barnea, Z., de Jonge, M. D., Dhal, B. B., Paterson, D., Cookson, D. & Chantler, C. T. (2003). *X-ray Spectrometry*, **32**, 69–74), **detector linearity** (Barnea, Z., Chantler, C. T., Glover, J. L., Grigg, M. W., Islam, M. T., de Jonge, M. D., Rae, N. A. & Tran, C. Q. (2011). *J. Appl. Cryst.* **44**, 281–6), **energy calibration** (Rae, N. A., Islam, M. T., Chantler, C. T. & de Jonge, M. D. (2010). Nucl. Instr. Meth. A, **619**, 147–149), **thickness calibration, bandwidth** (de Jonge, M. D., Barnea, Z. & Chantler, C. T. (2004). Phys. Rev. A, **69**, 022717–1 –12), but yields a highly accurate measurement of the coefficients with the correct scaling and relative amplitudes for processing using, for example, XERT for XAFS analysis (*Chantler, C. T. (2009). European Physical Journal ST*, **169**, 147–153; Chantler, C. T. (2010). *Rad. Phys. Chem.* 79, 117–123).

Slide 1 (top-left)

Harmonic Components

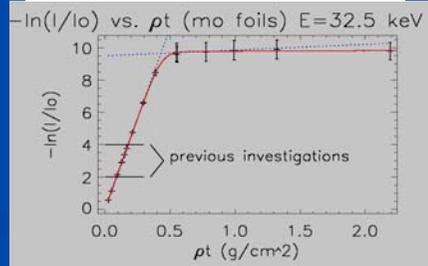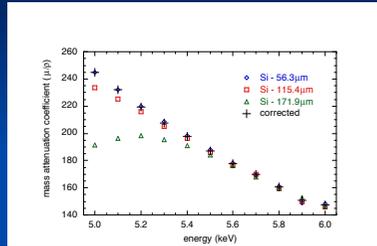3-foil measurement & signature for harmonic contamination

With a fraction x of harmonic photons in the beam

$$\ln(I/I_0) = \ln\left([1-x]e^{-[\mu/\rho]_F [\rho t]} + x e^{-[\mu/\rho]_H [\rho t]}\right)$$

APS, 1-ID 5th order undulator radiation, monochromated by a double-bounce silicon (311) monochromator, detuned to suppress higher order harmonics
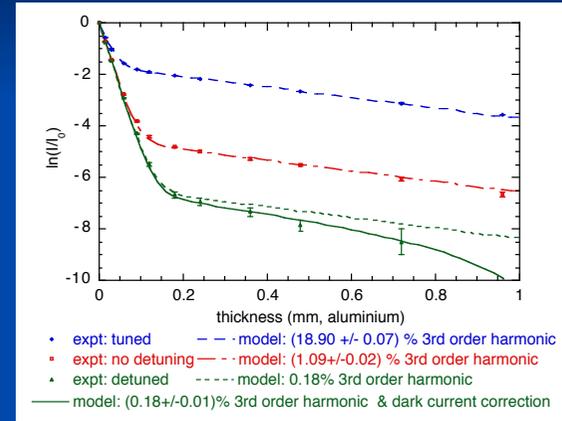
Tran, CQ, Barnea, Z, de Jonge, MD, Dhal, BB, Paterson, D, Cookson, D & Chantler, CT (2003). *X-ray Spectr*, **32**, 69–74

Harmonic Component $\leq e^{-9.5} \leq 1$ *in* 10^4 *photons*

molybdenum: measured values

$-\ln(I/Io)$ vs. ρt (mo foils) E=32.5 keV

previous investigations

Slide 2 (top-right)

Multiple-Foil Measurement & Effect of Tuning/Detuning

Detuning:
decrease harmonic component
decrease total incident flux

Tuning:
increase harmonic component
increase total incident flux

Optimisation:
minimise harmonic component without cutting too much flux

Multiple-foil measurement:
effective tool to quantitative investigation of harmonic component

- • expt: tuned   – – model: (18.90 +/- 0.07) % 3rd order harmonic
- • expt: no detuning   – · – model: (1.09+/-0.02) % 3rd order harmonic
- • expt: detuned   – – – model: 0.18% 3rd order harmonic
- —— model: (0.18+/-0.01)% 3rd order harmonic & dark current correction
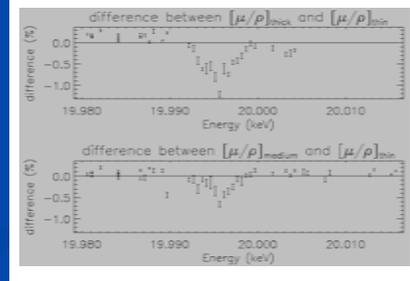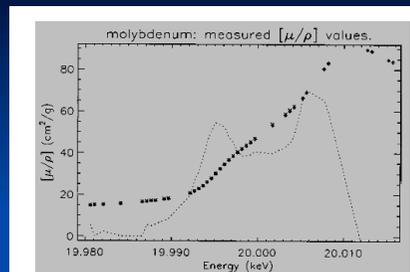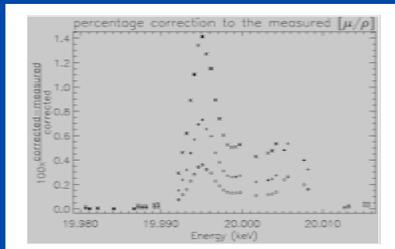
Slide 3 (bottom-left)

Bandwidth

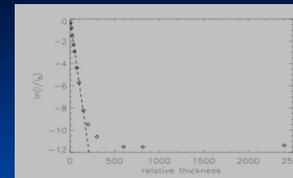*Effective beam monochromation:*
Synchrotron beam characterised:
1.57 eV ± 0.03 eV @ 20 keV

$[\mu/\rho]$ *corrected by 0.35%- 1.4%*

de Jonge, M. D., Barnea, Z. & Chantler, C. T. (2004). Phys. Rev. A, **69**, 022717–1 –12

molybdenum: measured $[\mu/\rho]$ values.

difference between $[\mu/\rho]_{thick}$ and $[\mu/\rho]_{thin}$

difference between $[\mu/\rho]_{medium}$ and $[\mu/\rho]_{thin}$

percentage correction to the measured $[\mu/\rho]$

Slide 4 (bottom-right)

The linearity of the data indicated by the dashed line shows
(i) the excellent linearity of the detection system &
(ii) no significant harmonic photons over a large attenuation range $0 > \ln(I/I_0) > -9$.

Barnea, Z., Chantler, C. T., Glover, J. L., Grigg, M. W., Islam, M. T., de Jonge, M. D., Rae, N. A. & Tran, C. Q. (2011). *J. Appl. Cryst.* **44**, 281–6

ideal measurements
$$\ln\frac{I}{I_0} = -\mu t$$
I, I_0: attenuated & incident intensities, respectively
μ: linear attenuation coeff. t: sample thickness

effect of harmonics
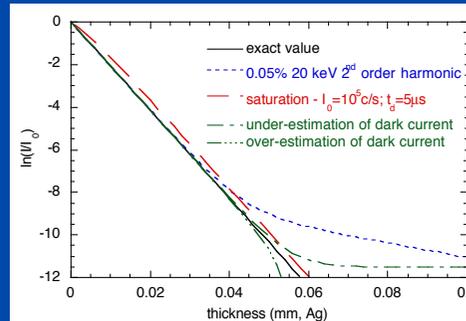$$\ln\left(\frac{I}{I_0}\right) = \ln\left[(1-x)e^{-\mu_f t} + x e^{-\mu_h t}\right]$$
x: fraction of harmonic
μ_f, μ_h: attenuation coeffs at fund. & harm. energies

effect of saturation
$$\ln\left(\frac{I}{I_0}\right) = \ln\left(\frac{\frac{I_T}{1+I_T t_d}}{\frac{I_{0,T}}{1+I_{0,T} t_d}}\right)$$
I_T, $I_{0,T}$: true count rates of attenuated & incident beams
t_D: dead time

dark current correction
$$\ln\left(\frac{I}{I_0}\right) = \ln\left(\frac{I - I_{off}}{I_0 - I_{0,off}}\right)$$
I_{off}, $I_{0,off}$: dark current correction for detectors

- —— exact value
- ······ 0.05% 20 keV 2nd order harmonic
- – · – saturation - $I_0 = 10^5$ c/s; $t_d = 5\mu s$
- – · – under-estimation of dark current
- – · · – over-estimation of dark current

Slide 1 (top-left)

Quantitative Investigation Of Current XAFS Analysis Techniques

Results - Standard Analysis [FEFF8.2]

8 Peak Window

Fitted Model XAFS Spectrum
Experimental XAFS Spectrum
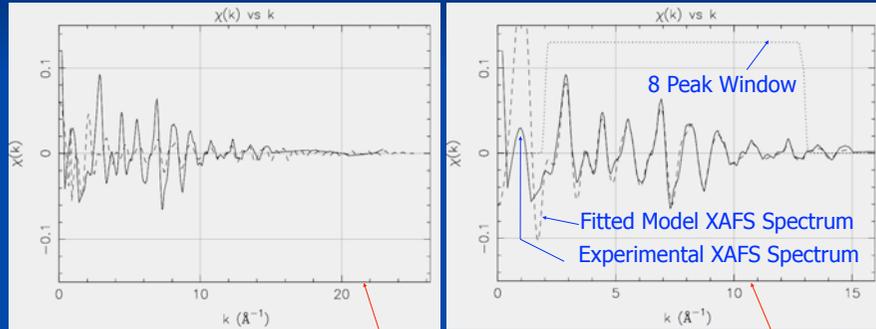
Smale, LF, Chantler, CT, de Jonge, MD, Barnea, Z & Tran, CQ (2006). Rad. Phys. Chem. **75**, 1559–1563.

Un-Windowed Fit of "Reduced Parameter Set"
χ_r^2 = 2500-3000

8 Peak Windowed Fit of "Reduced Parameter Set"
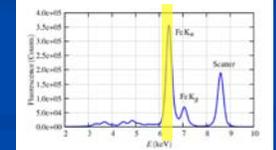χ_r^2 = 130

IUCr 2011. XAFS Tutorial. C.T. Chantler

Slide 2 (top-right)

3. How XAFS works - Realisation
B: Fluorescence [Chantler et al. sub.JSR 2011]

For fluorescence, to first order: $I_{f0} = f\,I_0\,(1 - \exp\{-[\mu/\rho][\rho t_p]\})$; I_{f0} : number of fluorescence photons, t_p: path length through the sample, f : fluorescence yield for the probability of producing a fluorescent photon (a K-α photon if the experiment is around the K-shell, or a L-shell photon if the experiment is around the L-shell etc.) after the process of photoabsorption and photoionisation (we should label $[\mu/\rho]$ with the subscript pe for the photoelectric effect only, and an asterisk indicating that only the component absorbed in the active centre producing a fluorescent photon is relevant - i.e. as $[\mu/\rho]^*_{pe}$). To first order, these fluorescent photons are emitted isotropically. Then

$$I_f = \frac{\frac{fI_0\Omega[\mu/\rho]^*_{pe}}{4\pi\cos\theta_{inc}}}{\frac{[\mu/\rho]}{\cos\theta_{inc}} + \frac{[\mu_f/\rho]}{\cos\theta_{out}}}\left(A - \exp\left(-\frac{\left[\frac{\mu}{\rho}\right][\rho t]}{\cos\theta_{inc}} - \frac{\left[\frac{\mu_f}{\rho}\right][\rho t]}{\cos\theta_{out}}\right)\right)$$

t is the depth of penetration into the material, Ω is the solid angle subtended by the detector channel, θ_{inc} is the angle of incidence of the incident X-ray (relative to the normal), θ_{out} is the angle of emission of the fluorescent X-ray (relative to the normal), $[\mu_f/\rho]$ is the mass attenuation coefficient of the material for the *fluorescent* photon energy; the integration constant A may be (loosely) estimated as $A = 1$. The number of fluorescent X-rays detected (in the region of interest) should include losses due to air path *air*, detector windows w etc. and detector quantum efficiencies overall ε as

N.b. I_f= F(ROI)

$$\frac{I_{f\,detected}}{I_{0\,monitored}} = \frac{I_f}{I_0}\left(\frac{\epsilon_{det}(E)}{\epsilon_{mon}(E)}\right)\exp\left(-\frac{\left[\frac{\mu_f}{\rho}\right]_{air}[\rho t_{air}]}{\cos\theta_{air}} - \frac{\left[\frac{\mu_f}{\rho}\right]_w[\rho t_w]}{\cos\theta_w}\right)$$

$t_{air}/\cos\theta_{air}$ is the path-length from the sample (surface) to the front face of the detector (window) and $t_w/\cos\theta_w$ is the path-length through a detector window of thickness t_w. Note the energy dependence of the relative efficiencies of the detectors.

IUCr 2011. XAFS Tutorial. C.T. Chantler

Slide 3 (bottom-left)

3. How XAFS works - Realisation
B: Fluorescence

$$I_f = \frac{\frac{fI_0\Omega[\mu/\rho]^*_{pe}}{4\pi\cos\theta_{inc}}}{\frac{[\mu/\rho]}{\cos\theta_{inc}} + \frac{[\mu_f/\rho]}{\cos\theta_{out}}}\left(A - \exp\left(-\frac{\left[\frac{\mu}{\rho}\right][\rho t]}{\cos\theta_{inc}} - \frac{\left[\frac{\mu_f}{\rho}\right][\rho t]}{\cos\theta_{out}}\right)\right)$$

$$\frac{I_{f\,detected}}{I_{0\,monitored}} = \frac{I_f}{I_0}\left(\frac{\epsilon_{det}(E)}{\epsilon_{mon}(E)}\right)\exp\left(-\frac{\left[\frac{\mu_f}{\rho}\right]_{air}[\rho t_{air}]}{\cos\theta_{air}} - \frac{\left[\frac{\mu_f}{\rho}\right]_w[\rho t_w]}{\cos\theta_w}\right)$$

For normal fluorescence XAFS geometries, the multi-element detector is placed at 90^0 to the incident beam, with the fluorescent sample, solid or solution, placed at an angle of 45^0 to the incident beam in order to minimise self-absorption. A particular detector channel will correspond to an emission angle θ_{out} which varies depending upon how close the sample stage is to the detector and its orientation etc. Similarly, the air path for the fluorescent X-ray to the detector, and the angle for the window attenuation, may then be given by

$$\theta_{w\,h} \simeq \theta_{air\,h} \simeq \theta_{out\,h} - 45^0$$

IUCr 2011. XAFS Tutorial. C.T. Chantler

Slide 4 (bottom-right)

3. How XAFS works - Realisation
B: Fluorescence

$$I_f = \frac{\frac{fI_0\Omega[\mu/\rho]^*_{pe}}{4\pi\cos\theta_{inc}}}{\frac{[\mu/\rho]}{\cos\theta_{inc}} + \frac{[\mu_f/\rho]}{\cos\theta_{out}}}\left(A - \exp\left(-\frac{\left[\frac{\mu}{\rho}\right][\rho t]}{\cos\theta_{inc}} - \frac{\left[\frac{\mu_f}{\rho}\right][\rho t]}{\cos\theta_{out}}\right)\right)$$

$$\frac{I_{f\,detected}}{I_{0\,monitored}} = \frac{I_f}{I_0}\left(\frac{\epsilon_{det}(E)}{\epsilon_{mon}(E)}\right)\exp\left(-\frac{\left[\frac{\mu_f}{\rho}\right]_{air}[\rho t_{air}]}{\cos\theta_{air}} - \frac{\left[\frac{\mu_f}{\rho}\right]_w[\rho t_w]}{\cos\theta_w}\right)$$

1) While the equation is a little complex, several components are fixed by geometry. If they are known, then the information content can be recovered effectively.
2) Absorption yields a straightforward relation from the log (I/I_0); this is not true for fluorescence.
3) If L is the distance from sample surface to detector, then $\Omega \simeq D/L^2$ where D is the area of the detector element.
4) θ_{out} varies across the detector & between detector channels. If detector channel centres are separated by a distance C and some central detector point is at 45^0 to the sample surface, then the angle of emission in the plane of incidence is $\theta_{out\,h} = 45^0 + \tan^{-1}(nC/L)$ where n is the number of channel elements from the central point. Due to misalignment, we should generalise this to $\theta_{out\,h} = \theta_0 + \tan^{-1}(nC/L)$. Different detector channels with different path-lengths will have strongly different self-absorption correction factors. Channels on the downstream side of the detector have approximately a single angle & a single self-absorption correction; those on the other side (upstream) have a much smaller self-absorption correction. Self-absorption is strongly energy-dependent especially due to $[\mu/\rho](E)$.
5) The pattern of the data expected from different channels can be fitted and corrected for self-absorption to provide a more robust data set with greater information content.
6) In many fluorescent geometries, square channel arrays are deliberately quite close to the sample stage to improve scattered fluorescent signals. Then the solid angle to a particular detector channel is important and we must use cos $\theta_{out} = \cos\theta_{out\,h}\cos\theta_{out\,v}$ where v is the vertical angle, which is zero in the plane of incidence. Then cos $\theta_{out\,v} = \tan^{-1}(mC/L)$ where m is the number of channel elements from the plane of incidence in the vertical axis.
7) Main parameters are θ_0 and L, allowing reduction of the whole equation to a consistent dataset with maximal information content.

IUCr 2011. XAFS Tutorial. C.T. Chantler

$$I_f = \frac{fI_0\Omega[\mu/\rho]^*_{pe}}{4\pi\cos\theta_{inc}}\left(A - \exp\left(-\frac{\left[\frac{\mu}{\rho}\right][\rho t]}{\cos\theta_{inc}} - \frac{\left[\frac{\mu_f}{\rho}\right][\rho t]}{\cos\theta_{out}}\right)\right)$$

$$\frac{I_{f_{detected}}}{I_{0monitored}} = \frac{I_f}{I_0}\left(\frac{\epsilon_{det}(E)}{\epsilon_{mon}(E)}\right)\exp\left(-\frac{\left[\frac{\mu_f}{\rho}\right]_{air}[\rho t_{air}]}{\cos\theta_{air}} - \frac{\left[\frac{\mu_f}{\rho}\right]_w[\rho t_w]}{\cos\theta_w}\right)$$

8) There are two particularly useful limits for fluorescence measurements. In the *thin sample limit* where $[\mu/\rho]\varrho t \ll 1$, the $1 - e^x$ term expands by Taylor series expansion, cancelling the denominator (and the self-absorption correction) so that

$$\frac{I_{f_{detected}}}{I_{0monitored}} = \frac{ft\Omega[\mu/\rho]^*_{pe}}{4\pi\cos\theta_{inc}}\frac{\epsilon_{det}(E)}{\epsilon_{mon}(E)}e^{-\frac{\left[\frac{\mu_f}{\rho}\right]_{air}[\rho t_{air}]+\left[\frac{\mu_f}{\rho}\right]_w[\rho t_w]}{\cos(\theta_{out h}-45^0)\cos\theta_{out v}}}$$

and to first order the observed intensity ratios are proportional to the photoelectric coefficient and the XAFS structure may be cleanly extracted. This *thin sample limit* is invalid whenever a dispersion between detector elements is observed - i.e. almost always.
9) The second convenient limit is the *thick dilute sample limit* where $[\mu/\rho]\varrho t \gg 1$ but $[\mu/\rho]_{pe} \ll [\mu/\rho]$ the exponential goes to zero yielding

$$\frac{I_{f_{detected}}}{I_{0monitored}} = \frac{\frac{f\Omega[\mu/\rho]^*_{pe}}{4\pi\cos\theta_{inc}}}{\frac{[\mu/\rho]}{\cos\theta_{inc}} + \frac{[\mu_f/\rho]}{\cos\theta_{out}}}\frac{\epsilon_{det}(E)}{\epsilon_{mon}(E)}e^{-\frac{\left[\frac{\mu_f}{\rho}\right]_{air}[\rho t_{air}]+\left[\frac{\mu_f}{\rho}\right]_w[\rho t_w]}{\cos(\theta_{out h}-45^0)\cos\theta_{out v}}}$$

Iff the energy dependence of the denominator is small (dominated by scattering coefficients or background absorption), then the angular self-absorption can be modelled and the corrected intensity ratio provides the photoelectric absorption coefficients for theoretical modelling using XAFS analysis. However, for most samples, the thin limit is not obeyed. Similarly, for most of the X-ray regime $[\mu/\rho]_{pe}$ is dominant and is not dominated by the scattering coefficients. For a typical metallic XAFS investigation, the concentration must be very low for $[\mu/\rho]^*_{pe}$ of the active fluorescent centre in the sample to be dominated by background absorption $[\mu/\rho]_{pe}$. Then of course the signal and statistical precision are also very low.
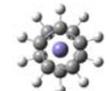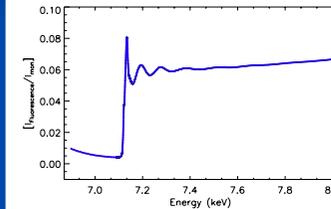
IUCr 2011. XAFS Tutorial. C.T. Chantler

10mM Ferrocene
Standard Fluorescence XAFS
Nobel Prize - sandwich compounds

D5h   D5d

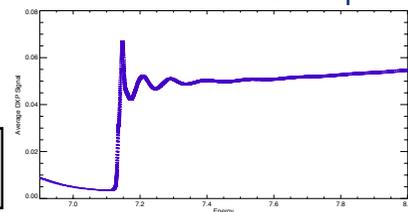Chantler et al., J Synch Rad, submitted   **IUCr 2011. XAFS Tutorial**. C.T. Chantler

---
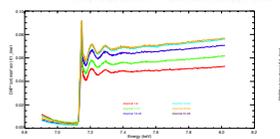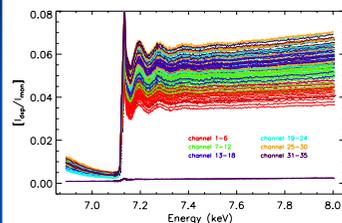
Single column dispersion
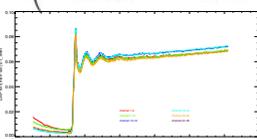
Corrected for self-absorption

10mM Ferrocene
3 scans, 35 pixels per scan
Fluorescence XAFS

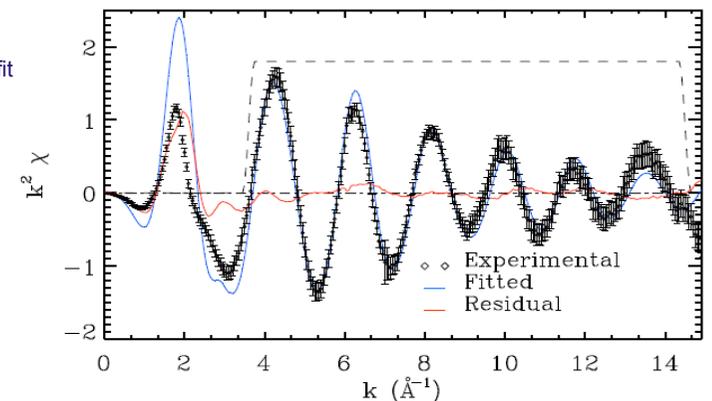Corrected XAFS Spectrum WITH ERROR BARS PROPAGATED

10mM Ferrocene
XAFS signal and fit
standard window

◇ Experimental
— Fitted
— Residual

Slide 1 (top-left)

3. How XAFS works
B: Fluorescence

Conformation	Eclipsed
Fitted Parameters	
χ_r^2	0.089
ΔE_0 offset (eV)	-1.72±0.94
$1 + \alpha$ scaling of lattice	1.0036±0.0037
σ^2 thermal parameter	0.0049±0.0013
S_0^2 amplitude reduction	1.069±0.086
Fixed Values	
Fe x,y,z,Å	0,0,0
C1(x,y,z)	1.6555,1.2007,0.0000
C2(x,y,z)	-1.6555,1.2007,0.0000
C3(x,y,z)	1.6555,-0.9714,0.7058
C4(x,y,z)	-1.6555,-0.9714,0.7058
C5(x,y,z)	1.6555,-0.9714,-0.7058
C6(x,y,z)	-1.6555,-0.9714,-0.7058
C7(x,y,z)	1.6555,0.3710,1.1420
C8(x,y,z)	-1.6555,0.3710,1.1420
C9(x,y,z)	1.6555,0.3710,-1.1420
C10(x,y,z)	-1.6555,0.3710,-1.1420
Derived Parameters including α scale uncertainty	
Fe-C$_5$,Å	1.6555(1.0036±0.0037)
Fe-C1,Å	2.045(1.0036±0.0037)
C-C,Å	1.4116(1.0036±0.0037)
Fe-C$_5$,Å	1.6615±0.0061
Fe-C1,Å	2.0524±0.0076
C-C,Å	1.4167±0.0052

Table 1: Fitted parameters

Slide 2 (top-right)

3. How XAFS works
B: Fluorescence

bond T lattice	XAFS Eclipsed 10K -	e-scattering[a]	Neutron[b] 173K	Xray[c] 98K Orthorhombic	Xray[d] 101K Triclinic	Xray[e] 173K Monoclinic	MP2[f]	CCSD/T[f]	This Study[g] Theory
Fe-C1,Å	2.0524±0.0076	2.064±0.003	±0.003-0.005	2.056,2.059±0.005	2.046,2.052±0.007	2.033-	1.910	2.056	2.065
range,Å	2.0524±0.0076	-	[2.005-2.050]	[2.051-2.062]	[2.041-2.052]	[2.017-2.048]			
C-C,Å	1.4167±0.0052	1.440±0.002	±0.005-0.009	1.429,1.431±0.006	1.426,1.433±0.007	1.395-	1.441	1.433	1.428
range,Å	1.4167±0.0052	-	[1.349-1.468]	[1.421-1.437]	[1.423-1.429]	[1.346-1.441]			
Fe-C$_5$,Å	1.6615±0.0061	1.660±0.003	-	1.658±0.006	1.646±0.007	1.651-	1.464	1.655	1.670

[a] (Haaland & Nilsson, 1968), [b] (Takusagawa & Koetzle, 1979), [c] (Seiler & Dunitz, 1982), [d] (Seiler & Dunitz, 1979b), [e] (Seiler & Dunitz, 1979a), [f] (Coriani et al., 2006), [g] the B3LYP/m6-31G model.
Table 2: Comparison of experimental bond lengths and theoretical predictions

Slide 3 (bottom-left)

4. Past, Present & Future: What is XERT?

The X-ray Extended Range Technique (XERT) is a method for measuring absorption and scattering to high accuracy.

Hence it can measure absorption coefficients, fluorescence signals and structures near absorption edges.

Like a detailed extended EXAFS (Extended X-ray Absorption Fine Structure).
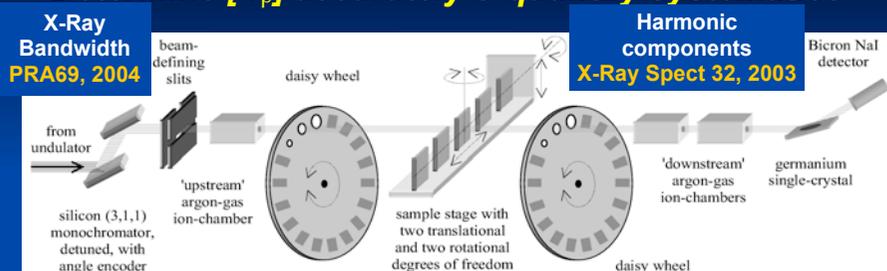
A few examples – highlights from 2008-2009

J. L. Glover, C. T. Chantler, Z. Barnea, N. A. Rae, C. Q. Tran, D. C. Creagh, D. Paterson, B. B. Dhal, 'High-accuracy measurements of the X-ray mass-attenuation coefficient and imaginary component of the form factor of copper,' Phys. Rev. A78 (2008) 052902

J. L. Glover, C. T. Chantler, 'Determination of the harmonic content of a synchrotron beam using X-ray attenuation measurements,' X-ray Spectr (2009)

J. L. Glover, C. T. Chantler, M. D. de Jonge, 'Nano-roughness in gold revealed from X-ray signature,' Phys. Lett. A373 (2009) 1177-1180

Slide 4 (bottom-right)

4. Past, Present & Future: How does it work?
Determine [μ/ρ] accurately & quantify systematics

X-Ray Bandwidth
PRA69, 2004

Harmonic components
X-Ray Spect 32, 2003

Optimisation of statistical level
X-Ray Spect 29, 2000

Sample thickness
Meas.Sci.&Technol.15, 2004
RSI 75, 2004

Fluorescence & scattering contributions
Rad.Phys.& Chem. 61, 2001
J.Phys.B37, 2004

Slide 1

- Independently calibrate monochromated energy
  - Avoid 3-10 eV or 30 -100 eV errors or offsets
- Energy is stepped commensurate with structure
  - Finer grid near edges
- Multiple thickness foils for each energy
- Measurements of multiple apertures for each foil
- For each foil-aperture: sample, blank, dark current
- Repeat each measurement e.g. 10 times
- Measure harmonic contamination (daisy wheels)
- Detailed materials characterisation / profiling

Slide 2

Uses _multiple foils_, and investigates _extended ranges_ in experimental parameters (_energy_; _attenuation_ - $0.5 \leq \ln(I_0/I) \leq 6$; _collimation_...)

- **requires synchrotron radiation**
- **individual systematics identified, minimised & corrected for**
- **Harmonic test:**

$0.02 \leq \ln(I_0/I) \leq 20$!

Slide 3
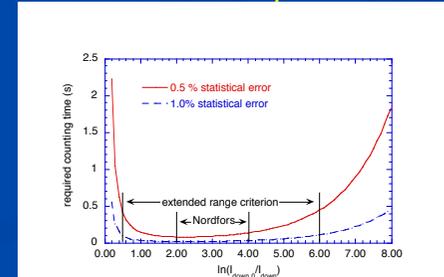
Normalisation of signals for dark current and common paths

$$\ln\left(\frac{\left(\dfrac{I_2 - dc_2}{I_1 - dc_1}\right)_{sample+air}}{\left(\dfrac{I_2 - dc_2}{I_1 - dc_1}\right)_{air}}\right)$$

$$= \ln\left(\frac{A_2 Y_2 E_2 e^{-(\mu t)_{IC1}} e^{-(\mu t)_{sample}} e^{-(\mu t)_{air}}}{A_1 Y_1 E_1}\Bigg/\frac{A_2 Y_2 E_2 e^{-(\mu t)_{IC1}} e^{-(\mu t)_{air}}}{A_1 Y_1 E_1}\right)$$
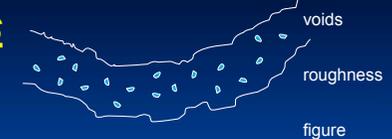
$$= -(\mu t)_{sample}$$

with: A = amplification
 Y = electron yield per x-ray absorbed
 E = Ion Chamber efficiency
 dc = dark current measurement
 I = Ion Chamber measured current
 1, 2 = upstream / downstream ion chamber

Slide 4

XAFS Theory: XANES and EXAFS Spectra
Sample Thickness

voids
roughness
figure

Since:

$$\frac{\mu}{\rho} = \frac{1}{-\rho t}\ln\left(\frac{I}{I_o}\right)$$
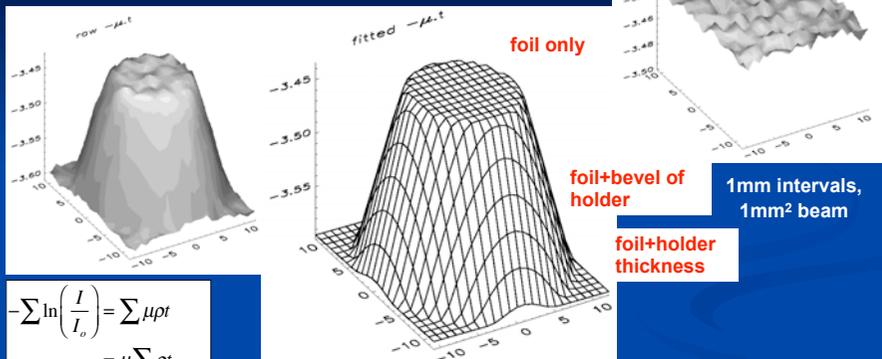
$$\%\sigma_{[\mu/\rho]} = \%\sigma_{\rho t}$$

micrometry:
$\pm 1\mu m \Rightarrow 4\%\text{-}0.4\%$
error for 25-250 μm
samples

mass / area:

$$(\rho t)_{av} = {}^{mass}/_{Area}$$

$$(\sigma_{\rho t})_{av} = 0.01 \text{ - } 0.03\ \%$$

local **thickness may differ by ~5% from this value**

Slide 1 (top-left)

Full-foil Mapping of Solids:

foil only

foil+bevel of holder

foil+holder thickness

1mm intervals, 1mm² beam

$$-\sum \ln\left(\frac{I}{I_o}\right) = \sum \mu \rho t$$
$$= \mu \sum \rho t$$
$$= \mu (\rho t)_{total}$$
$$= \mu \left(\frac{m}{A}\right) n_x n_y$$
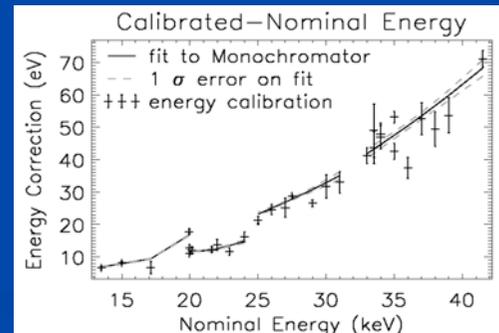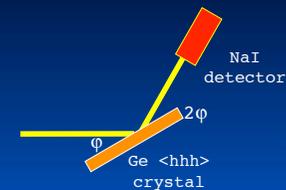
μ & $(\rho t)_{local}$ *quantified to <0.03%*

X-ray mapping gives *high precision* of *correct* local structure (integrated column density) and a *rigorous link* to the absolute average

Slide 2 (top-right)

Energy Calibration (example)

to get $\frac{\Delta \mu}{\mu} \leq 0.1\%$,

$\Delta E \leq 2.5 - 10\,\mathrm{eV}$ at $E = 10 - 40\,\mathrm{keV}$

energy calibration every ~1-2 keV
111, 333, 444, 555, 777, …, -1-1-1,…

7-70 eV (±1-3 eV)

modification to stated synchrotron energies.

XAFS : 0.1 eV desirable but reference lines determined only to 0.3 -3 eV

NaI detector

2φ

φ

Ge <hhh> crystal

Calibrated−Nominal Energy

— fit to Monochromator
-- 1 σ error on fit
+++ energy calibration

Energy Correction (eV)

Nominal Energy (keV)

Slide 3 (bottom-left)

XAFS Theory: XANES and EXAFS Spectra
Roughness, σ

voids

roughness

figure

only significant when roughness(σ) ~ t
affects attenuation according to:
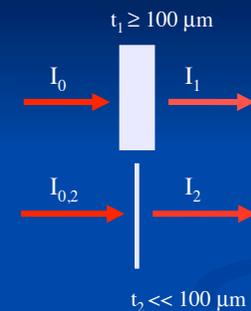
$$\frac{I}{I_0} = e^{-\mu t}\left\{1 + \frac{\mu^2 \sigma^2}{2!} + ...\right\}$$

this gives a μ dependent systematic.

Roughness characterisation, thickness transfer and the XERT can be used to characterise this source of error

Slide 4 (bottom-right)

XAFS Theory: XANES and EXAFS Spectra
Thickness transfer scheme for thin foils

$t_1 \geq 100\,\mu m$
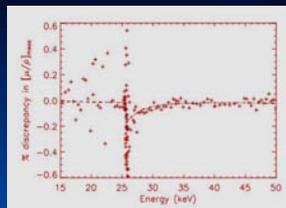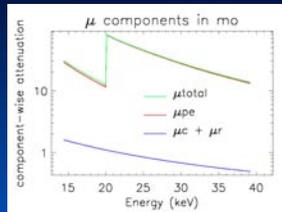
I_0 I_1

$I_{0,2}$ I_2

$t_2 \ll 100\,\mu m$

$\%\sigma_{t,\,local} \leq 0.1\%$

$$t_{eff} = \frac{1}{\mu}\ln\left(\frac{I_0}{I}\right) \Rightarrow t_{2,eff} = t_{1,eff}\ln\left[\frac{\left(I_{0,2}/I_2\right)}{\left(I_0/I_1\right)}\right]$$

Four issues in Scattering:


$[^{\mu}/_{\rho}]_{pe}$ *corrected by 0.04%- 0.3%*

1. Observation of scattering & fluorescence in transmission
2. Major issues in recent literature & conferences:
3. *I: Coherent vs incoherent elastic scattering: Bragg Diffraction vs Rayleigh vs Thermal Diffuse Scattering. Problems in theory & experiment.*
4. *II: How to do XAFS with different coherence?*
5. *III: Can we measure the absolute coefficient for scattering (doubly-differential or in any form)?*
6. *IV: Photoelectron Inelastic Scattering: Significance for XAFS interpretation and theory*
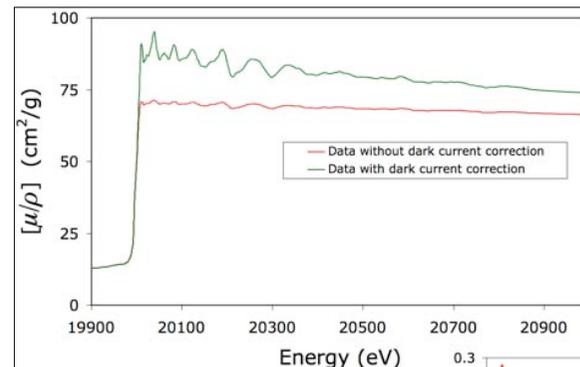
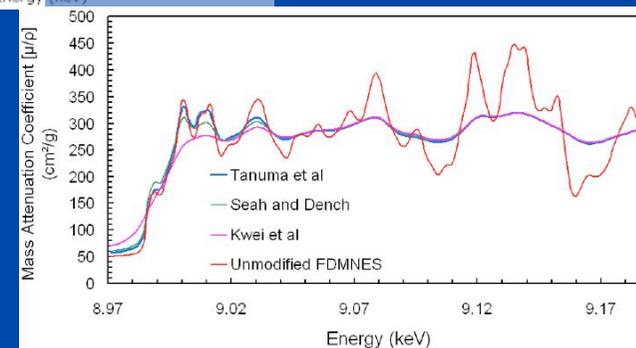How accurate is conventional XAFS?
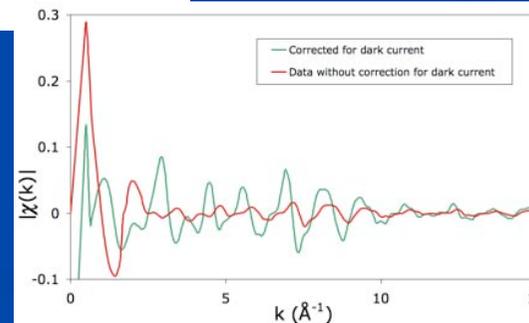
XAFS
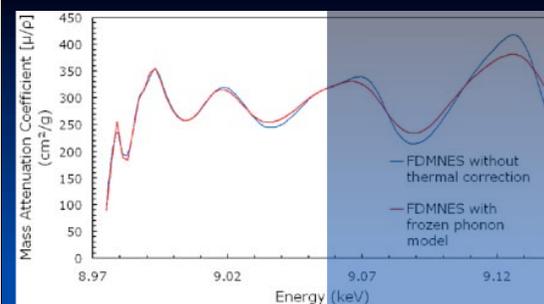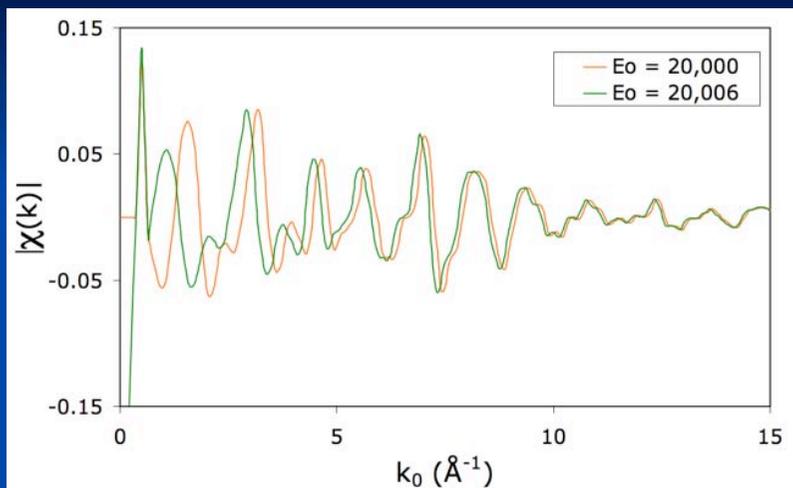
Influence of temperature

New implementation of T for FDM

First application of FDM to XAFS

Influence of inelastic mean free path:
Alternate theory tested

Slide 1 (top-left)

XAFS Theory: XANES and EXAFS Spectra

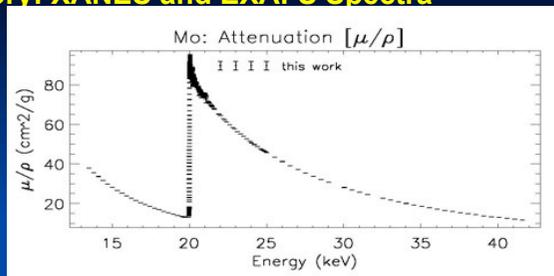**_Accuracy:_**
_0.02% - 0.15 %_

Mo: Attenuation [μ/ρ]

TABLE II: Error contributions to the values reported in Table I, with source specified. Further established limits for the systematic uncertainty are quoted here.
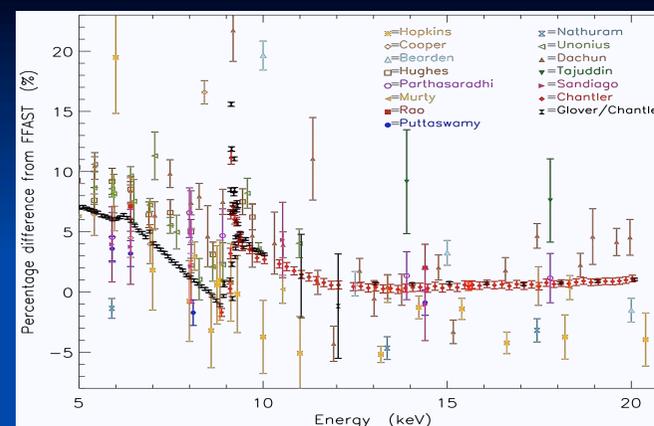
IUCr 2011. XAFS Tutorial. C.T. Chantler

Slide 2 (top-right)

What kinds of questions?

1. Investigating Fermi levels, bound-bound transitions, shake processes, temperature factors, inelastic mean free paths, XANES, XAFS
2. Ideal solids (silicon, copper, …)
3. Simple (or complex) binary systems: (ZnSe, CdS, SiO_2…)
- Room Temperature *[and cold]* studies of phases and coordination (like XAFS, XANES): e.g. 4-coordinated Ni complexes
- *[Elevated (High-T, high-P)]* Phases and coordination of metallic complexes in solution
- Organometallics and catalysts
- Reaction kinetics; Bioactive centres; Biomedical
- **Challenges:**
- XERT accuracies & methodology for Fluorescence (Scattering) studies
- XERT accuracies & methodology for High-T solutions
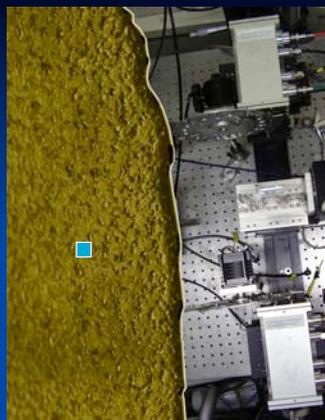
Slide 3 (bottom-left)

4. Past, Present & Future: Developments of theory

- Extensions of the Finite Difference Method for Near Edge Structure (FDMNES) have been employed to calculate X-ray Absorption Fine Structure (XAFS)
- thermal vibrations under a correlated Debye-Waller model
- finite photoelectron inelastic mean free path
- computed over 300 eV above the K edge, >2x the greatest energy range previously reported for a solid state calculation using this method
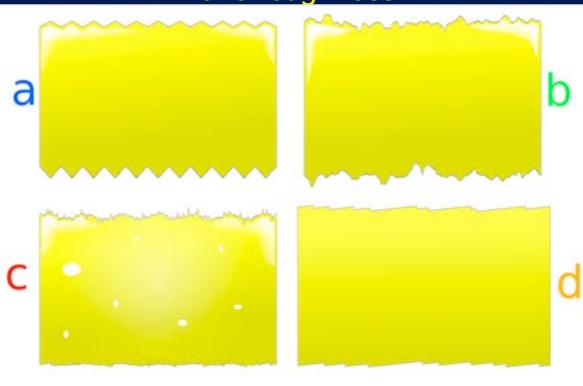- Cf muffin-tin approaches

Slide 4 (bottom-right)

Copper

J. L. Glover, C. T .Chantler, Z. Barnea, N. A. Rae, C. Q. Tran, D. C. Creagh, D. Paterson, B. B. Dhal, 'High-accuracy measurements of the X-ray mass-attenuation coefficient and imaginary component of the form factor of copper,' Phys. Rev. A78 (2008) 052902

Slide 1

a b c d

J. L. Glover, C. T. Chantler, M. D. de Jonge, 'Nano-roughness in gold revealed from X-ray signature,' Phys. Lett. A373 (2009) 1177-1180

Slide 2

epoxidation catalysts in the Ni-catalysed polymerisation of isocyanides:

Activated complex, $C_{3l}H_{53}Cl_2N_5NiO_8$ tri(tert-pentyl isocyanide) [benzylamino(tertpentylamino) carbene] nickel(II) perchlorate

[Glover et al. AIP Proc. CP882/ XAFS13 (2007) 625]
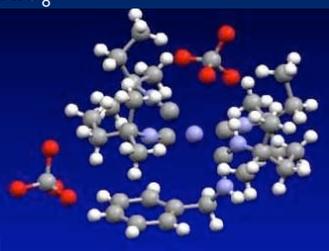

Slide 3
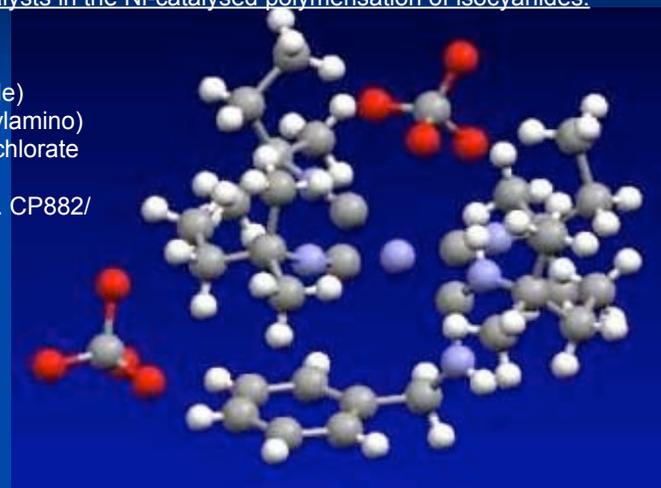
Activated complex, $C_{3l}H_{53}Cl_2N_5NiO_8$ tri(tert-pentyl isocyanide) [benzylamino(tertpentylamino) carbene] nickel(II) perchlorate [Glover et al. AIP Proc. CP882/ XAFS13 (2007) 625]
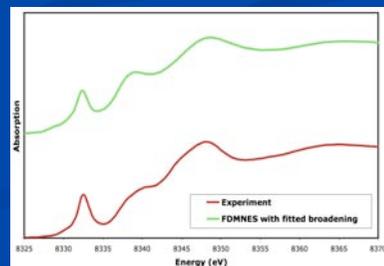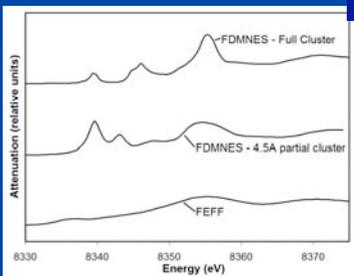
Muffin-Tin Potential: Poor approx. for near edge structure

FDMNES: good for near edge structure

Slide 4

Key Challenges for the Future?

- 1. XAFS using **fluorescence** (& energy dispersive detection) – treatment of self-absorption & statistics; **phases** with temperature
- 2. **dilute non-crystalline systems**: glasses, polymers, composites, solutions – maximum (sufficient?) information content cf noise level
- 3. development of **routine** experimental setup, analysis & processing for conventional users
- 4. **data uncertainties** & **propagation of errors**
- 5. development of DHF & **condensed matter theory** – preferably for XAFS & XANES

New synchrotron techniques & applications

New techniques at synchrotrons can drive higher accuracy, structural information and insight in traditional fields such as XAFS [1-5], XANES and powder diffraction [6], & initiate new fields including those of nanoroughness measurement [7], measurement of electron inelastic mean free paths [8,9], bonding information at an accuracy of crystallographic determination [10], & advances for fluorescence and scattering investigations.

[1] C. Q. Tran, C. T. Chantler, Z. Barnea, Physical Review Letts 90 (2003) 257401-1-4

[2] M. D. de Jonge, C. Q. Tran, C. T. Chantler, Z. Barnea, B. B. Dhal, D. J. Cookson, W.-K. Lee, A. Mashayekhi,' Phys. Rev. A 71, 032702 (2005)

[3] J. L. Glover, C. T .Chantler, Z. Barnea, N. A. Rae, C. Q. Tran, D. C. Creagh, D. Paterson, B. B. Dhal, Phys. Rev. A78 (2008) 052902

[4] N. A. Rae, C. T. Chantler, Z. Barnea, M. D. de Jonge, C. Q. Tran, J. R. Hester, Phys. Rev. A 81 (2010) 022904-1-10

[5] M. T. Islam, N. A. Rae, J. L. Glover, Z. Barnea, M. D. de Jonge, C. Q. Tran, J. Wang, and C. T. Chantler, Phys. Rev. A 81 (2010) 022903-1-9

[6] C. T. Chantler, C. Q. Tran, D. J. Cookson, 'Precise measurement of the lattice spacing of LaB_6 standard powder by the x-ray extended range technique using synchrotron radiation', Phys. Rev. A69 (2004) 042101-1 -11

[7] J. L. Glover, C. T. Chantler, M. D. de Jonge, 'Nano-roughness in gold revealed from X-ray signature,' Phys. Lett. A373 (2009) 1177-1180

[8] J. D. Bourke, C .T. Chantler, Measurements of Electron Inelastic Mean Free Paths in Materials, Phys. Rev. Letters 104 (2010) 206601-1-4

[9] J. D. Bourke, C .T. Chantler, X-ray Spectroscopic Measurement of the Photoelectron Inelastic Mean Free Paths in Molybdenum, Journal of Physical Chemistry Letters (2010) acc

[10] J. L. Glover, C. T. Chantler, Z. Barnea, N. A. Rae, C. Q. Tran, J. Phys. B 43 (2010) 085001-1-15

New synchrotron techniques & applications
Team: Melbourne (& elsewhere)

Experimental: **Chris Chantler, Zwi Barnea, Chanh Tran [La Trobe], Martin de Jonge [ASRP Medal, AS], Nicholas Rae, Barbara Etschmann [Adelaide], Jack Glover, Justin Kimpton [AS], Tauhid Islam**

Collaborations & earlier students:

David Cookson, David Paterson, David Balaic

James Hester [ANSTO], Dudley Creagh [Canberra, IUCr], Bipina Dhal

Stephen Southworth, Linda Young, Elliot Kanter

Eireann Cosgriff, Garry Foran, Stephen Best (Chemistry),

Joel Brugger (Earth Sciences), Chris Ryan (CSIRO), other DP, LIEF...

Support & Encouragement: *John Hubbell [NIST],* **Dudley Creagh**

Theory: **Chris Chantler, Lucas Smale, Jack Glover, Jay Bourke, Chris Witte, Andrew Hayward, John Lowe**

Recent Students: **Emile Janssons, Gerard Atkinson, Lachlan Tantau**

Acknowledgement: Theory: **Yves Joly [ESRF]**

XAFS Theory: XANES and EXAFS Spectra

Developments of theory

- Extensions of the Finite Difference Method for Near Edge Structure (FDMNES) have been employed to calculate X-ray Absorption Fine Structure (XAFS)

- thermal vibrations under a correlated Debye-Waller model

- finite photoelectron inelastic mean free path

- computed over 300 eV above the K edge, >2x the greatest energy range previously reported for a solid state calculation using this method

- Cf muffin-tin approaches

IUCr 2011. XAFS Tutorial. C.T. Chantler
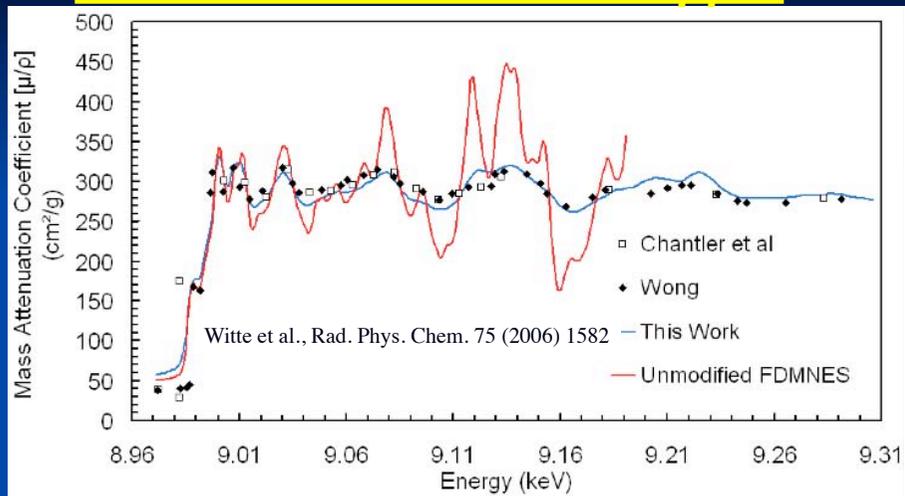

New synchrotron techniques & applications

FINITE DIFFERENCE STRUCTURE COMPUTATIONS FOR XANES - AND XAFS

- **J. D. BOURKE, C. T. CHANTLER, C. WITTE, 'Finite Difference Method Calculations of X-ray Absorption Fine Structure for Copper,' Physics Letters A, 360 (2007), 702-706**

- **J. D. Bourke, C. T. Chantler, 'Finite difference method calculations of long-range X-ray absorption fine structure for copper over k ~ 20 A^{-1},' NIM A619 (2010) 33-36**

- **Y Joly: FDMNES**

DEVELOPMENTS OF FEFF, IFFEFIT etc.:

- **J. J. Kas, J. J. Rehr, J. L. Glover, C. T. Chantler, Comparison of Theoretical and Experimental Cu and Mo K-edge XAS, NIM A619 (2010) 28-32**

- **L. F. SMALE, C. T. CHANTLER, M. D. DE JONGE, Z. BARNEA, C.Q. TRAN, `Analysis of X-ray Absorption Fine Structure using Absolute X-ray Mass Attenuation Coefficients: Application to Molybdenum,' Radiation Physics & Chemistry 75 (2006) 1559-1563**
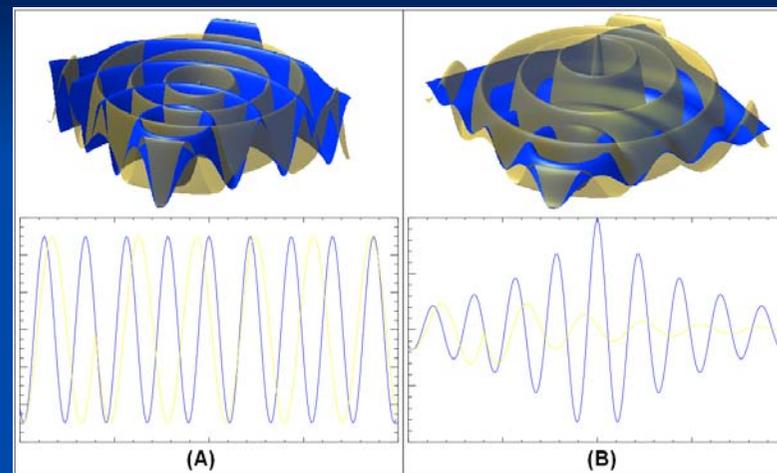
Solid State Structure - Copper

Witte et al., Rad. Phys. Chem. 75 (2006) 1582

- □ Chantler et al
- ◆ Wong
- — This Work
- — Unmodified FDMNES

NO fitting parameter: **accurate** experiment and **accurate** theory **CAN** agree!
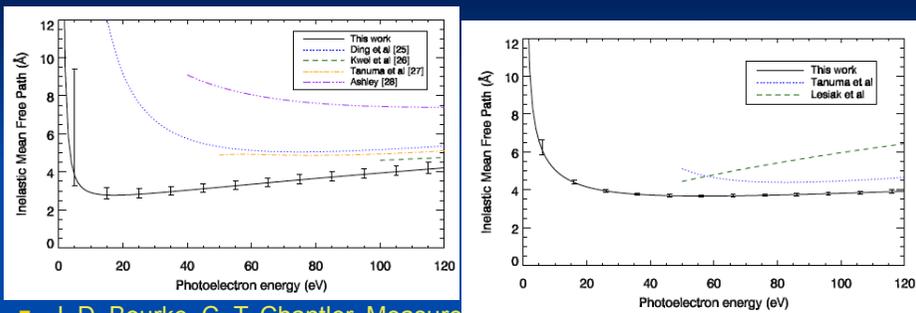
New synchrotron techniques & applications

INELASTIC MEAN FREE PATHS from XAFS

(A)   (B)

New synchrotron techniques & applications

INELASTIC MEAN FREE PATHS from XAFS

- J. D. Bourke, C .T. Chantler, Measurements of Electron Inelastic Mean Free Paths in Materials, Phys. Rev. Letters 104 (2010) 206601-1-4
- C .T. Chantler, J. D. Bourke, X-ray Spectroscopic Measurement of the Photoelectron Inelastic Mean Free Paths in Molybdenum, Journal of Physical Chemistry Letters 1 (2010) 2422-2427
- MS76 Sunday & many other presentations at this congress.